

Potts Partition Function Zeros and Ground State Entropy on Hanoi Graphs

Shu-Chiuan^a Chang and Robert Shrock^b

(a) *Department of Physics*

National Cheng Kung University,

Tainan 70101, Taiwan and

(b) *C. N. Yang Institute for Theoretical Physics and*

Department of Physics and Astronomy

Stony Brook University, Stony Brook, NY 11794

We study properties of the Potts model partition function $Z(H_m, q, v)$ on m 'th iterates of Hanoi graphs, H_m , and use the results to draw inferences about the $m \rightarrow \infty$ limit that yields a self-similar Hanoi fractal, H_∞ . We also calculate the chromatic polynomials $P(H_m, q) = Z(H_m, q, -1)$. From calculations of the configurational degeneracy, per vertex, of the zero-temperature Potts antiferromagnet on H_m , denoted $W(H_m, q)$, estimates of $W(H_\infty, q)$, are given for $q = 3$ and $q = 4$ and compared with known values on other lattices. We compute the zeros of $Z(H_m, q, v)$ in the complex q plane for various values of the temperature-dependent variable $v = y - 1$ and in the complex y plane for various values of q . These are consistent with accumulating to form loci denoted $\mathcal{B}_q(v)$ and $\mathcal{B}_v(q)$, or equivalently, $\mathcal{B}_y(q)$, in the $m \rightarrow \infty$ limit. Our results motivate the inference that the maximal point at which $\mathcal{B}_q(-1)$ crosses the real q axis, denoted q_c , has the value $q_c = (1/2)(3 + \sqrt{5})$ and correspondingly, if $q = q_c$, then $\mathcal{B}_y(q_c)$ crosses the real y axis at $y = 0$, i.e., the Potts antiferromagnet on H_∞ with $q = (1/2)(3 + \sqrt{5})$ has a $T = 0$ critical point. Finally, we analyze the partition function zeros in the y plane for $q \gg 1$ and show that these accumulate approximately along parts of the sides of an equilateral triangular with apex points that scale like $y \sim q^{2/3}$ and $y \sim q^{2/3}e^{\pm 2\pi i/3}$. Some comparisons are presented of these findings for Hanoi graphs with corresponding results on m 'th iterates of Sierpinski gasket graphs and the $m \rightarrow \infty$ limit yielding the Sierpinski gasket fractal.

I. INTRODUCTION

Studies of iteratively defined hierarchical graphs G_m with the property that the limiting graph G_∞ is a self-similar fractal have produced many interesting results in physics and mathematics (some reviews include [1]-[4]). There have been a number of studies of spin models and critical phenomena on fractals, e.g., [5]-[31]. A spin model of particular interest is the Potts model [32–34]. On a lattice, or, more generally, on a graph G , in thermal equilibrium at temperature T , the partition function for the Potts model is

$$Z = \sum_{\{\sigma_i\}} e^{-\beta\mathcal{H}} , \quad (1.1)$$

where $\beta = 1/(k_B T)$, k_B is the Boltzmann constant, and the Hamiltonian is

$$\mathcal{H} = -J \sum_{e_{ij}} \delta_{\sigma_i \sigma_j} , \quad (1.2)$$

where J is the spin-spin interaction constant, i and j denote vertices (= sites) in G , e_{ij} is the edge (= bond) connecting them, and σ_i are classical spins taking on values in the set $\{1, \dots, q\}$. We use the notation

$$K = \beta J , \quad y = e^K , \quad v = y - 1 . \quad (1.3)$$

We denote the partition function of the Potts model on a graph G as $Z(G, q, v)$. This function is equivalent to an important graph-theoretic function, the Tutte polynomial, as will be reviewed in Section II. For the Potts antiferromagnet (PAF), $J < 0$ so that, as $T \rightarrow 0$, $K \rightarrow -\infty$; hence, in this limit (where $v \rightarrow -1$), the only contributions to the PAF partition function are from spin configurations in which adjacent spins have different values. The resultant $T = 0$ PAF partition function is therefore precisely the chromatic polynomial $P(G, q)$ of the graph G , which counts the number of ways of assigning q colors to the vertices of G , subject to the condition that no two adjacent vertices have the same color. An important feature of the antiferromagnetic Potts model is that for sufficiently large q on a given graph G with finite maximal vertex degree, it has a nonzero entropy per site at zero temperature, $S_0 = k_B \ln W$, where W denotes the ground state degeneracy per site. This is important as an exception to the third “law” of thermodynamics, that the entropy per site vanishes at zero temperature. A physical example of this phenomenon is the residual entropy of ice [35]-[38].

A standard way to define a fractal is to start with some initial graph G_0 and then apply a procedure to construct a related graph with more vertices and edges, forming the $m = 1$

iterate, G_1 , so forth with G_2 , etc. By continuing this process in an iterative manner, one produces a graph G_m , the m 'th iterate in the given hierarchical family. In the cases of interest here, in the limit $m \rightarrow \infty$, the resultant object, denoted G_∞ , is self-similar, often with a non-integer Hausdorff dimension, whence the term ‘‘fractal’’. Two graph iterates whose $m \rightarrow \infty$ limits yield fractals are the m 'th iterates of the Sierpinski gasket graph, S_m , and of the Hanoi graph, H_m . Sierpinski gasket iterates were studied in some of the earliest papers on spin models on fractals [6]-[8]. Mathematical studies of Hanoi graphs include, e.g., [39]-[41]. The first few iterates of Hanoi graphs are shown below, using a common labelling convention in which the initial graph is labelled $m = 0$. (Some authors use a different labelling convention in which the initial graph is denoted $m' = 1$, so $m' = m + 1$.)

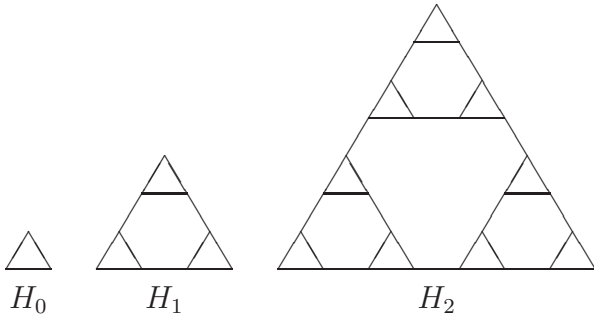


FIG. 1. Initial Hanoi graph H_0 and first two iterates, H_1 and H_2

In this paper we study properties of the Potts model partition function $Z(H_m, q, v)$ of m 'th iterates of Hanoi graphs, H_m . We make use of an iterative procedure for calculating the equivalent Tutte polynomial derived by Donno and Iacono in Ref. [24]. We also calculate the chromatic polynomials $P(H_m, q) = Z(H_m, q, -1)$. From calculations of the configurational degeneracy per vertex for the q -state Potts antiferromagnet, denoted $W(H_m, q)$, for $q = 3$ and $q = 4$, for a large range of m , we extrapolate to $m \rightarrow \infty$ to obtain estimates of $W(H_\infty, 3)$ and $W(H_\infty, 4)$, and compare these with known values on other lattices. We calculate zeros of $Z(H_m, q, v)$ in the q plane for various values of v and zeros of $Z(H_m, q, v)$ in the v plane for various values of q , including results up to $m = 4$. Our focus is primarily on the chromatic zeros, i.e., the zeros in the complex q plane for $v = -1$, corresponding to the zero-temperature Potts antiferromagnet. From our calculations, we are able to draw plausible inferences concerning properties of the respective accumulation sets of zeros in these respective planes in the limit $m \rightarrow \infty$, denoted $\mathcal{B}_q(v)$ and $\mathcal{B}_v(q)$, or equivalently, $\mathcal{B}_y(q)$,

where $y = v + 1$. As will be discussed in detail below, our results motivate the inference that for $v = -1$ (the zero-temperature Potts antiferromagnet), the maximal point at which $\mathcal{B}_q(v)$ crosses the real- q axis, denoted q_c , has the value $q_c = (1/2)(3 + \sqrt{5})$, and correspondingly, if $q = q_c$, then $\mathcal{B}_v(q_c)$ crosses the real v axis at $v = -1$. Results are also given for zeros of $Z(H_m, q, v)$ in the q plane for the finite-temperature Potts antiferromagnet and ferromagnet. Furthermore, we analyze the partition function zeros in the y plane for several values of q and for $q \gg 1$ and determine the general behavior of the large- q zeros. In previous work, we have calculated partition function zeros on m 'th iterates of the Sierpinski gasket graph, and at appropriate points we will make comparisons with our earlier results on Sierpinski gasket graphs. In addition to studies of spin models on m 'th iterates of hierarchical graphs, calculations of several graph-theoretic quantities, such as the number of spanning trees, spanning forests, connected spanning subgraphs, etc. have been computed on Sierpinski and Hanoi graphs; some of these computations were presented in [42]-[54].

II. SOME BACKGROUND

In this section we briefly review some relevant background on graph theory, the Potts model partition function, Tutte polynomials, and Hanoi graphs. In general, a graph $G = (V, E)$ is defined by its set of vertices (sites), V , and its set of edges (bonds), E . We denote the number of vertices in G as $n = n(G) = |V|$ and the number of edges in G as $e(G) = |E|$. The degree Δ_{v_i} of a vertex $v_i \in V$ is defined as the number of edges that connect to this vertex. The number of connected components of a graph, each of which is disjoint from the others, is denoted $k(G)$. The girth g of a graph G is the number of edges in a minimal-length closed circuit in G . The cyclomatic number of G , i.e., the number of linearly independent circuits in G , denoted $c(G)$, and satisfies the relation $c(G) = e(G) + k(G) - n(G)$. A graph $G' = (V, E')$ is a spanning subgraph of a graph $G = (V, E)$ if it has the same vertex set and its edge set is a subset of the edge set of G , i.e., $E' \subseteq E$ [55, 56].

A. Potts Model Partition Function and Tutte Polynomial

As defined in Eqs. (1.1) and (1.2), the number of states of a given classical spin in the Potts model is a positive integer, q . An important generalization of this starts with an expression for the Potts model partition function $Z(G, q, v)$ on a graph G as a sum of

contributions from spanning subgraphs $G' \subseteq G$ [33], which reads

$$Z(G, q, v) = \sum_{G' \subseteq G} q^{k(G')} v^{e(G')} , \quad (2.1)$$

where $k(G')$ and $e(G')$ denote the number of connected components and edges of G' . Since $k(G') \geq 1$ and $e(G') \geq 0$, $Z(G, q, v)$ is a polynomial in q and v (of degree $n(G)$ in q and of degree $e(G)$ in v). The physical range of v in the Potts ferromagnet (FM, $J > 0$) is $0 \leq v \leq \infty$, corresponding to $\infty \geq T \geq 0$, while in the Potts antiferromagnet (AFM, $J < 0$), it is $-1 \leq v \leq 0$ corresponding to $0 \leq T \leq \infty$. In the ferromagnetic case, Eq. (2.1) allows one to extend the definition of q from the positive integers \mathbb{Z}_+ to the positive real numbers \mathbb{R}_+ while maintaining $Z(G, q, v) > 0$ and hence a Gibbs measure. One can formally also consider this extension for the antiferromagnetic case, although in this case, if q is not a positive integer, it is not guaranteed that $Z(G, q, v)$ is positive, since $v < 0$. For the Potts antiferromagnet, since $J < 0$, as $T \rightarrow 0$, $K \rightarrow -\infty$ and $v \rightarrow -1$; as noted in the introduction, in this limit, the resultant $T = 0$ partition function is the chromatic polynomial $P(G, q)$ of the graph G [55]-[57]:

$$Z(G, q, -1) = P(G, q) . \quad (2.2)$$

This coloring is called a proper q -coloring of (the vertices of) G . The minimum value of q for which one can perform a proper q -coloring of a graph G is the chromatic number of G , denoted $\chi(G)$.

On a given graph G , the ground state (i.e., zero-temperature) degeneracy per vertex of the Potts antiferromagnet is

$$W(G, q) = [P(G, q)]^{1/n(G)} . \quad (2.3)$$

With physically relevant values of q , $P(G, q)$ is positive, and one uses the canonical real positive n 'th root in this evaluation. For the $n(G) \rightarrow \infty$ limit of a given family of graphs G , we formally denote

$$\{G\} = \lim_{n(G) \rightarrow \infty} G . \quad (2.4)$$

The ground state degeneracy per vertex of the Potts antiferromagnet in this limit is

$$W(\{G\}, q) = \lim_{n(G) \rightarrow \infty} [P(G, q)]^{1/n(G)} , \quad (2.5)$$

and the corresponding ground state entropy per site is

$$S_0(\{G\}, q) = k_B \ln[W(\{G\}, q)] . \quad (2.6)$$

As discussed in [58, 59], for certain values of q , denoted q_s , one must take account of the noncommutativity

$$\lim_{n(G) \rightarrow \infty} \lim_{q \rightarrow q_s} [P(G, q)]^{1/n(G)} \neq \lim_{q \rightarrow q_s} \lim_{n(G) \rightarrow \infty} [P(G, q)]^{1/n(G)} . \quad (2.7)$$

The special values of q_s here include $q \in \{0, 1, 2\}$ since $P(H_m, q)$ vanishes at these values. Because the calculations of $W(H_m, q)$ that we present in this paper are for $q > 2$, either order of limits can be used for these calculations.

For a general graph G , the Potts model partition function is equivalent to an important function in mathematical graph theory, the Tutte polynomial, $T(G, x, y)$ [60]-[63]. The Tutte polynomial can be expressed as a sum of contributions from spanning subgraphs $G' \subseteq G$ as

$$T(G, x, y) = \sum_{G' \subseteq G} (x - 1)^{k(G') - k(G)} (y - 1)^{c(G')} . \quad (2.8)$$

Since $k(G') - k(G) \geq 0$ and $c(G') \geq 0$, this is, indeed, a polynomial in x and y . The equivalence between $Z(G, q, v)$ and $T(G, x, y)$ is

$$\begin{aligned} Z(G, q, v) &= (x - 1)^{k(G)} (y - 1)^{n(G)} T(G, x, y) \\ &= (q/v)^{k(G)} v^{n(G)} T(G, x, y) , \end{aligned} \quad (2.9)$$

where

$$x = 1 + \frac{q}{v} \quad (2.10)$$

and

$$y = v + 1 = e^K . \quad (2.11)$$

where K was defined in Eq. (1.3). Note that

$$q = (x - 1)(y - 1) . \quad (2.12)$$

Special cases of the Tutte polynomial yield a number of important one-variable polynomials, including the chromatic polynomial, flow polynomial, and reliability polynomial. In particular, the special case $x = 1 - q$, $y = 0$ yields the chromatic polynomial:

$$P(G, q) = (-q)^{k(G)} (-1)^{n(G)} T(G, 1 - q, 0) . \quad (2.13)$$

B. Hanoi Graphs

We recall some elementary properties of the H_m hierarchical graphs. The initial graph H_0 is a triangle graph, $K_3 = C_3$, where K_n and C_n are respectively, the complete graph and the circuit graph with n vertices. With the commonly used labelling convention for m 'th iterates that we follow, the number of vertices in the m 'th iterate Hanoi graph is

$$n(H_m) = 3^{m+1} , \quad (2.14)$$

and the numbers of edges in H_m is

$$e(H_m) = \frac{3(3^{m+1} - 1)}{2} . \quad (2.15)$$

The cyclomatic number of H_m is thus

$$c(H_m) = \frac{3^{m+1} - 1}{2} . \quad (2.16)$$

The number of faces of H_m , denoted $N_F(H_m)$, is

$$N_F(H_m) = \frac{3^{m+1} - 1}{2} , \quad (2.17)$$

which is equal to $c(H_m)$. The number of triangular faces in H_m , denoted $N_t(H_m)$, is

$$N_t(H_m) = 3^m . \quad (2.18)$$

Consequently, in the limit $m \rightarrow \infty$, the ratio of the number of triangular faces to the total number of faces is

$$\lim_{m \rightarrow \infty} \frac{N_t(H_m)}{N_F(H_m)} = \frac{2}{3} . \quad (2.19)$$

A Δ -regular graph G is defined as a graph with the property that all of its vertices have the same degree, Δ . In a Δ -regular graph, one has the relation $\Delta = 2e(G)/n(G)$. Even if a graph is not Δ -regular, one can still define an effective vertex degree in the $n(G) \rightarrow \infty$ limit as

$$\Delta_{\text{eff}} = \lim_{n(G) \rightarrow \infty} \frac{2e(G)}{n(G)} . \quad (2.20)$$

In a Hanoi graph H_m , the three vertices forming the original H_0 triangle have vertex degree 2, while all of the other vertices have vertex degree 3. Hence,

$$\Delta_{\text{eff}}(H_\infty) = 3 . \quad (2.21)$$

Since there are some similarities of Hanoi graphs and Sierpinski graphs, it is useful to compare and contrast our new results on zeros of $Z(H_m, q, v)$ with our previous results for the zeros of $Z(S_m, q, v)$, where S_m denotes the m 'th iterate Sierpinski gasket graph. For the reader's convenience, we list some relevant properties of m 'th iterates of Sierpinski gasket graphs in Appendix B.

III. CALCULATIONS AND RESULTS

A nonlinear iterative procedure for calculating the Tutte polynomial $T(H_m, x, y)$ of the m 'th Hanoi graph iterate, H_m , in terms of contributions from lower- m -order iterates, was given by Donno and Iacono in [24] and is briefly described in Appendix A. (See also [30] for a different approach.) Using this nonlinear iterative method of Ref. [24], we have calculated $T(H_m, x, y)$ and the equivalent $Z(H_m, q, v)$ for $0 \leq m \leq 4$. From Eq. (2.2) or equivalently (2.13), we have computed $P(H_m, q)$ for these values of m . The results for the initial graph H_0 are elementary, since $H_0 = K_3 = C_3$, so $T(H_0, x, y) = x + x^2 + y$; $Z(H_0, q, v) = (q + v)^3 + (q - 1)v^3$; and $P(H_0, q) = q(q - 1)(q - 2)$. We have used a different method to calculate the values of chromatic polynomials and hence ground state entropy per vertex for certain values of q of particular interest, namely $q = B_5$ (see Eq. (5.7)), $q = 3$, and $q = 4$; for these calculations; instead of having to compute the full chromatic polynomial $P(H_m, q)$ for arbitrary q and then substitute a special value of q , we set q equal to this value at the outset in the iterative computation, which thus involves just integer arithmetic or powers of elements of the algebraic number field $\mathbb{Q}[\sqrt{5}]$. (Here the algebraic number field $\mathbb{Q}[\sqrt{t}]$ is the field of elements of the form $r + s\sqrt{t}$, where $r, s, t \in \mathbb{Q}$ and t is not a perfect square.) These computations for fixed integers or algebraic numbers can be carried to considerably higher values of m , as will be discussed in Section IV.

We first discuss our results for the chromatic polynomials $P(H_m, q)$. We find the following general structural formula for $m \geq 1$ that describes the $P(H_m, q)$ that we have calculated:

$$P(H_m, q) = q(q - 1)(q - 2)^{3m} Q_m(q) \quad \text{for } m \geq 1, \quad (3.1)$$

where $Q_m(q)$ is a polynomial of degree

$$\deg(Q_m(q)) = 3^{m+1} - 3m - 2. \quad (3.2)$$

For $m = 1$ we observe a simple factorization

$$\begin{aligned} Q_1(q) &= q^4 - 5q^3 + 10q^2 - 10q + 5 \\ &= \frac{1}{4} \left[2q^2 - (5 + \sqrt{5})q + (5 + \sqrt{5}) \right] \left[2q^2 - (5 - \sqrt{5})q + (5 - \sqrt{5}) \right]. \end{aligned} \quad (3.3)$$

The polynomial $Q_2(q)$ that occurs in $P(H_2, q)$ is

$$Q_2(q) = q^{19} - 26q^{18} + 322q^{17} - 2528q^{16} + 14125q^{15} - 59771q^{14}$$

$$\begin{aligned}
& + 198981q^{13} - 534267q^{12} + 1176423q^{11} - 2147675q^{10} + 3271840q^9 \\
& - 4170694q^8 + 4444555q^7 - 3940970q^6 + 2880770q^5 - 1709450q^4 \\
& + 803125q^3 - 286075q^2 + 70750q - 9500 ,
\end{aligned} \tag{3.4}$$

In [30], $P(H_m, q)$ was given for m up to 2 (with our labelling convention, which is equivalent $m' = 3$ in the labelling convention of Ref. [30]), and our results agree. We have calculated $P(H_m, q)$ for higher m in a similar manner. From our results, we can observe several interesting properties of $P(H_m, q)$ and its zeros, as well as drawing plausible inferences for features of $P(H_\infty)$, from these results.

In addition to the structural property (3.1), one may investigate factorizations of $P(H_m, q)$ (and thus $Q_m(q)$) for specific values of q . As an example, we take $q = 3$ and $q = 4$. We find that the values of $P(H_m, q)$ do not, in general, have simple factorizations; for example,

$$P(H_3, 3) = 2^{13} \cdot 3 \cdot (233) \cdot (32002057) \tag{3.5}$$

and

$$P(H_3, 4) = 2^{24} \cdot 3 \cdot (34471) \cdot (67883) \cdot (12983) \cdot (167772879347) . \tag{3.6}$$

In contrast, in [23] we found that $P(S_m, 3) = 3! \forall m$ and that $P(S_m, 4)$ has simple factorizations as displayed in Eq. (4.5) below.

IV. GROUND STATE DEGENERACY OF POTTS ANTIFERROMAGNET ON HANOI GRAPHS

From our calculations of the ground state degeneracy per vertex for the Potts antiferromagnet on the Hanoi iterates, H_m , for a range of m , we can extrapolate to $m \rightarrow \infty$ to obtain estimates of $W(H_\infty, q)$. For reference, we show values of $W(H_m, q)$ in Table I for our inferred value of $q_c(H_\infty) = B_5$, (see Eq. (5.1)) and for the next two integral values of q , namely $q = 3$ and $q = 4$. (Here and below, numbers in floating-point format are listed to the indicated number of significant figures.) Because the integer arithmetic involved in the evaluation of $P(H_m, 3)$ and $P(H_m, 4)$ is exact, while the evaluation of $P(H_m, B_5)$, involving powers of the irrational quantity $q = B_5 = (1/2)(3 + \sqrt{5})$, requires a floating-point evaluation, we are able to obtain accurate evaluations of $W(H_m, 3)$ and $W(H_m, 4)$ over a large range of m , namely $0 \leq m \leq 16$, while we conservatively retain our evaluations of $W(H_m, q)$ for $q = B_5$ only

up to $m = 12$. Although we thus limit the listings in Table I to $0 \leq m \leq 12$, there is very little change in $W(H_m, q)$ going from $m = 12$ to $m = 16$ for $q = 3$ and $q = 4$, as is evident from $W(H_{16}, 3) = 1.4887646$ versus $W(H_{12}, 3) = 1.4887651$, and $W(H_{16}, 4) = 2.4991903$ versus $W(H_{12}, 4) = 2.4991909$. In Ref. [30], values of $W(H_m, q)$ were given for $0 \leq m \leq 7$ (corresponding to $1 \leq m' \leq 8$ in the labelling convention of [30]) and for some integral values of q . For the range of m where our values of $W(H_m, 3)$ and $W(H_m, 4)$ can be compared with those in [30], they agree, and ours extend to higher m . We find that for the values of m and q for which we have performed these calculations, $W(H_m, q)$ is a monotonically decreasing function of m for fixed q . We consider the large- m limit for two (integral) values of q where comparison can be made with results for the zero-temperature q -state Potts antiferromagnet on regular lattices, namely $q = 3$ and $q = 4$. Extrapolating to the $m = \infty$ limit, we obtain $W(H_\infty, 3) = 1.489(1)$ and $W(H_\infty, 4) = 2.499(1)$, where the estimated uncertainties are indicated in parentheses.

It is of interest to compare these estimates with values of $W(\{G\}, q)$ for $n \rightarrow \infty$ limits of various families of graphs. There have been many calculations of $W(\{G\}, q)$ and lower and upper bounds on this quantity for various families of graphs, e.g., [35]-[38], [64]-[98] and later works (see [99] for some references). Some calculations have been carried out for hierarchical graphs G_m leading to fractals in the $m \rightarrow \infty$ limit in works including [23, 28, 29]. As background for comparisons, we remark on a general property of $W(\{G\}, q)$. In the assignment of colors to a given vertex of a graph, the constraint that this vertex must have a color that is different from each adjacent vertex is more restrictive as the number of adjacent vertices increases. If the graphs in a family are Δ -regular, then this number of adjacent vertices is given by Δ . Even if the graphs in a family are not Δ -regular, since we focus here on the $n(G) \rightarrow \infty$ limit, we may use Δ_{eff} as a measure of the number of adjacent vertices. Because the restriction on the proper q -coloring of the vertices becomes more severe as Δ increases, it follows that this reduces the ground state degeneracy, i.e., $W(\{G\}, q)$ is a decreasing function of Δ (or Δ_{eff} if finite- n graphs are not Δ -regular). This monotonic dependence was shown in Fig. 5 of [58] for the honeycomb (hc), square (sq), and triangular (tri) lattices. Since the coloring freedom is greater for larger q , one naturally starts with $q \gg 1$ and moves to smaller values of q in analyzing $W(\{G\}, q)$ for a particular limit $\{G\}$. The analytic form of $W(\{G\}, q)$ is the same along the real- q axis until q decreases to $q_c(\{G\})$. Therefore, if one compares $W(\{G\}, q)$ for different $\{G\}$, and, in particular, different regular lattices Λ , then the monotonicity comparison can be made for the interval of q larger than the largest $q_c(\{G\})$ among the $\{G\}$ being compared. For these lattices, one knows the integral values $q_c(\text{tri}) = 4$ [68, 69], $q_c(\text{sq}) = 3$ [37, 38], and, formally, $q_c(\text{hc}) = (1/2)(3 + \sqrt{5})$ [103, 104]. Thus, for the comparison, one takes the interval $q \geq 4$. Over this interval, the

TABLE I. Values of the ground state degeneracy per vertex of the Potts antiferromagnet on the m 'th Hanoi iterate, H_m , for $q = (1/2)(3 + \sqrt{5})$, $q = 3$, and $q = 4$, denoted $W(H_m, B_5)$, $W(H_m, 3)$, and $W(H_m, 4)$. Values are listed for $0 \leq m \leq 12$

m	$W(H_m, B_5)$	$W(H_m, 3)$	$W(H_m, 4)$
0	1.378241	1.817121	2.884499
1	1.185301	1.592838	2.6219375
2	1.123589	1.522681	2.539454
3	1.103741	1.499985	2.512540
4	1.097203	1.492495	2.503632
5	1.095033	1.490007	2.500670
6	1.094310	1.489179	2.499683
7	1.094069	1.488903	2.499355
8	1.093989	1.488811	2.499245
9	1.093962	1.488780	2.4992085
10	1.0939535	1.488770	2.499196
11	1.093951	1.488766	2.499192
12	1.093950	1.488765	2.499191

results in this Fig. 5 of [58] show that for a fixed q , $W(hc, q) > W(sq, q) > W(tri, q)$. This set of inequalities is in accord with the fact that $\Delta(hc) < \Delta(sq) < \Delta(tri)$.

Since $\Delta_{\text{eff}} = 3$ for H_∞ , we first compare our estimates of $W(H_\infty, 3)$ and $W(H_\infty, 4)$ with $W(\{G\}, q)$ with $q = 3, 4$ for $n(G) \rightarrow \infty$ limits $\{G\}$ of several Δ -regular families of graphs with the same vertex degree, $\Delta = 3$. This comparison is shown in Table II. From the discussion in the previous paragraph, one expects that, for a given q in the interval larger than the largest $q_c(\{G\})$ among the limits $\{G\}$ being compared, $W(H_\infty, q)$ should be similar to $W(\{G\}, q)$ for other $\{G\}$ with the same Δ or Δ_{eff} , and the comparison in Table II is in agreement with this expectation. We comment on the entries in Table II as follows. The values of $W(hc, 3)$ and $W(hc, 4)$ are from high-precision Monte Carlo simulations performed for [73] and [74]. The actual Monte Carlo (MC) results given in [73, 74] (with uncertainties

TABLE II. Values of $W(\{G\}, 3)$ and $W(\{G\}, 4)$ for various $n(G) \rightarrow \infty$ limits of families of graphs and regular lattices G that have $\Delta = 3$ or $\Delta_{\text{eff}} = 3$. The quantity $g(G)$ is the girth.

$\{G\}$	$g(G)$	$W(\{G\}, 3)$	$W(\{G\}, 4)$
H_∞	3	1.489(1)	2.499(1)
Λ_{488}	4	1.686	2.622
sq, $2_F \times \infty$	4	1.732	2.646
hc	6	1.660	2.604

in parentheses) are $W(hc, 3) = 1.6600(5)$ and $W(hc, 4) = 2.6038(7)$. In Table II we also list a comparison with $W(\Lambda_{488}, q)$ with $q = 3, 4$. The actual values computed from MC simulations for Ref. [74] are $W(\Lambda_{488}, 3) = 1.68575(60)$ and $W(\Lambda_{488}, 4) = 2.62226(75)$. Here, Λ_{488} is an Archimedean lattice comprised of squares and octagons. We recall the definition of an Archimedean lattice, as a uniform tiling of the plane by regular polygons in which all vertices are equivalent. Such a lattice is specified by the ordered sequence of polygons that one traverses in making a complete circuit around a vertex in a given (say counterclockwise) direction. This is incorporated in the mathematical notation for an Archimedean lattice, $(\prod_i p_i^{a_i})$, where in the above circuit, the notation $p_i^{a_i}$ indicates that the regular polygon with p_i sides occurs contiguously a_i times; it can also occur noncontiguously. Thus, the Λ_{488} lattice is the Archimedean lattice such that when one makes a circuit in the local neighborhood of any vertex, one traverses a square, and then two octagons. In Table II we also list values of $W(\{G\}, q)$ with $q = 3, 4$ for the infinite-length limit of the strip of the square lattice with width $L_y = 2$ vertices and free transverse boundary conditions (which is independent of the longitudinal boundary conditions), for which [58]

$$W(sq, 2_F \times \infty, q) = (q^2 - 3q + 3)^{1/2}. \quad (4.1)$$

Hence, $W(sq, 2_F \times \infty, 3) = \sqrt{3} = 1.7320508..$ and $W(sq, 2_F \times \infty, 4) = \sqrt{7} = 2.6457513..$ (In the case of periodic longitudinal boundary conditions, this is a Δ -regular graph, while in the case of longitudinal boundary conditions, one uses Δ_{eff} , and these are both equal to 3.) We also note that for the Diamond Hierarchical Lattice (DHL), with $\Delta_{\text{eff}} = 3$ (and girth 4), denoting the m 'th iterate as D_m , Ref. [29] obtained $W(D_\infty, 3) = \sqrt{3} = 1.7320508..$, which again is similar to the value of $W(H_\infty, 3)$.

We may also compare our inferred values of $W(H_m, 3)$ and $W(H_m, 4)$, as well as our

estimates of $W(H_\infty, 3)$ and $W(H_\infty, 4)$, with values for the Sierpinski gasket, with $\Delta_{\text{eff}} = 4$. For the m 'th iterate S_m of this family of hierarchical graphs,

$$P(S_m, q = 3) = 3! \tag{4.2}$$

so that

$$W(S_\infty, q = 3) = 1 . \tag{4.3}$$

One has

$$P(S_0, q = 4) = 24 = 2^3 \cdot 3 \tag{4.4}$$

and in [23], for $m \geq 1$, we obtained

$$P(S_m, q = 4) = 2^{3^{m+3}} \cdot 3^{3^{m-1}} , \tag{4.5}$$

so that in the limit $m \rightarrow \infty$, the ground state (i.e., zero-temperature) degeneracy per site for the Potts antiferromagnet on S_∞ is

$$W(S_\infty, q = 4) = 2^{2/3} \cdot 3^{2/9} = 2.026346 , \tag{4.6}$$

in agreement with Ref. [19], where $W(S_\infty, q = 4)$ had been obtained earlier. The approach to this asymptotic limit is shown by the specific values for $W(S_m, 3)$ and $W(S_m, 4)$ listed in Table III. As is evident from Table III, these values converge reasonably rapidly toward their respective $m \rightarrow \infty$ values. Our values of $W(H_m, 3)$ and $W(H_m, 4)$ in Table I also show reasonably rapid convergence, which led to the quoted uncertainties in our extrapolations to estimate the values of $W(H_\infty, 3)$ and $W(H_\infty, 4)$.

In general, for the values of m for which we have calculated $W(H_m, q)$ and $W(S_m, q)$, we find the inequality for $m \geq 1$

$$W(H_m, q) > W(S_m, q) \quad \text{if } m \geq 1 \quad \text{and } q \geq 3 , \tag{4.7}$$

The restriction to $m \geq 1$ is made here because $W(H_0, q) = W(S_0, q)$, as a consequence of the fact that the initial graph for both S_m and H_m iterates is the same, namely a triangle: $S_0 = H_0 = K_3$. The inequality (4.7) reflects the above-mentioned property that, for a fixed $q > q_c(\{G\})$, $W(\{G\}, q)$ is a monotonically decreasing function of the vertex degree Δ or, where applicable, the effective vertex degree Δ_{eff} . Here, the inequality can be understood since the fractal H_∞ has a smaller value of Δ_{eff} , namely 3, compared with S_∞ , for which $\Delta_{\text{eff}} = 4$. Presuming that (4.7) holds for arbitrarily large m , it implies that in the $m \rightarrow \infty$ limit,

$$W(H_\infty, q) \geq W(S_\infty, q) \quad \text{for } q \geq 3 , \tag{4.8}$$

and again, one expects this to be realized as a strict equality.

TABLE III. Values of the ground state degeneracy per vertex of the Potts antiferromagnet on S_m for $q = 3$ and $q = 4$, denoted $W(S_m, 3)$ and $W(S_m, 4)$, with $0 \leq m \leq 12$, for comparison with the values of $W(H_m, 3)$ and $W(H_m, 4)$ in Table I.

m	$W(S_m, 3)$	$W(S_m, 4)$
0	1.817121	2.884499
1	1.348006	2.401874
2	1.126878	2.1689435
3	1.043584	2.076164
4	1.014674	2.043221
5	1.0049075	2.032002
6	1.001638	2.028235
7	1.000546	2.026976
8	1.000182	2.026556
9	1.000061	2.026416
10	1.000020	2.026369
11	1.000007	2.026354
12	1.000002	2.026349
∞	1	2.026346

V. CHROMATIC ZEROS OF H_m

In this section we study the zeros of $P(H_m, q) = Z(H_m, q, -1)$, i.e., the chromatic zeros of H_m . In Figs. 2-4 we show plots of the zeros of $P(H_m, q)$ in the complex q plane for $2 \leq m \leq 4$. As is evident, the complex zeros form a roughly oval shape centered approximately at $q = 1$. It may be recalled that for an arbitrary graph, a chromatic polynomial has the following zero-free regions on the real axis: (i) $(-\infty, 0)$, (ii) $(0, 1)$ [100], and (iii) $(1, \frac{32}{27})$ [101, 102]. The chromatic polynomials $P(H_m, q)$ always have zeros at $q = 0$, $q = 1$, and $q = 2$. Most of the zeros have positive real parts, although some zeros on the left-hand part of the locus with nonzero imaginary parts have small negative real parts, i.e., lie in the second and third

quadrants.

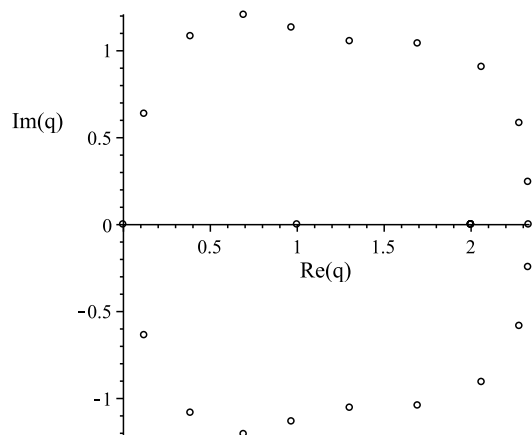


FIG. 2. Zeros of the chromatic polynomial $P(H_2, q)$ in the q plane.

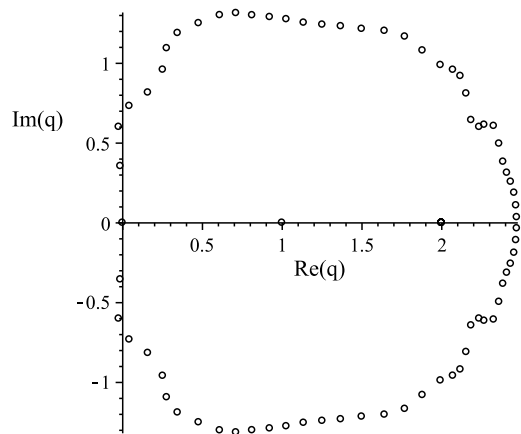


FIG. 3. Zeros of the chromatic polynomial $P(H_3, q)$ in the q plane.

We denote the locus of zeros of $Z(H_m, q, v)$ in the limit $m \rightarrow \infty$ (i) in the complex q plane for a given v as $\mathcal{B}_q(v)$ and (ii) in the complex v plane for a given q as $\mathcal{B}_v(q)$. Since we only discuss the chromatic zeros of H_m in this section, we will use the simpler notation for the asymptotic locus $\mathcal{B}_q(-1) = \mathcal{B}_q$, with $v = -1$ being understood implicitly. In a manner similar to our earlier study of zeros of the partition function for Sierpinski gasket graphs in Ref. [23], our study here of chromatic zeros for a range of m , allows us to draw some

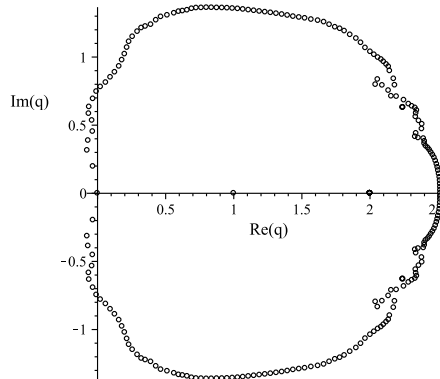


FIG. 4. Zeros of the chromatic polynomial $P(H_4, q)$ in the q plane.

TABLE IV. Values of largest real (lr) zero or largest real part (lrp) of the complex-conjugate pair of zeros of $P(H_m, q)$ for $0 \leq m \leq 4$, with extrapolated value in the $m \rightarrow \infty$ limit. For comparison with $B_5 = (1/2)(3 + \sqrt{5})$, we list the respective fractional differences $FD = (B_5 - q_{lr})/B_5$ or $FD = (B_5 - q_{lrp})/B_5$ in the third column.

m	q_{lr} or q_{lrp}	FD
0	2 (lr)	0.236068
1	2 (lr)	0.236068
2	2.331734 (lr)	0.109357
3	2.472039 (lrp)	0.055765
4	2.517208 (lrp)	0.038512

plausible inferences about the $m \rightarrow \infty$ limit. In particular, we infer that \mathcal{B}_q crosses the real- q axis at $q = 0$ and at a maximal point which we denote q_c . For finite m , we denote the largest real (lr) zero of $P(H_m, q)$ as q_{lr} . For certain m , the zeros of $P(H_m, q)$ include a complex-conjugate pair characterized by a small imaginary part and a real part that is larger than any other real zeros or the real parts of other complex-conjugate pairs of zeros. We label the real parts of these complex-conjugate pairs with the abbreviation (lrp), standing for “largest real part”.

An extrapolation of these results leads to the inference that in the $m \rightarrow \infty$ limit,

$$q_c(H_\infty) = \frac{3 + \sqrt{5}}{2} = 2.618034 . \quad (5.1)$$

The complex-conjugate pairs whose real parts are listed in Table 5.1 are

$$m = 3 : \quad q = 2.472039 \pm 0.0349188i \quad (5.2)$$

and

$$m = 4 : \quad q = 2.517208 \pm 0.0225300i . \quad (5.3)$$

Our use of the real parts of these complex-conjugate pairs to get information relevant to q_c is motivated by the fact that they are quite close to the real axis; the ratios of the magnitude of the respective imaginary parts divided by the real parts are 0.0141255 for $m = 3$ and 0.008950 for $m = 4$, decreasing as m increases. Our inferred value of $q_c(H_\infty)$ in Eq. (5.1) is related to the well-known golden mean ϕ

$$\phi = \frac{1 + \sqrt{5}}{2} = 1.618034 \quad (5.4)$$

satisfying $\phi^2 = \phi + 1$. Namely,

$$q_c(H_\infty) = \phi + 1 . \quad (5.5)$$

It is also of interest to observe that our inferred value of $q_c(H_\infty)$ is equal to a Tutte-Beraha number, namely

$$q_c(H_\infty) = B_5 , \quad (5.6)$$

where

$$B_r = 4 \cos^2 \left(\frac{\pi}{r} \right) . \quad (5.7)$$

Note that for any finite m , B_5 cannot be a chromatic zero of H_m or, indeed, any graph. We recall the elementary proof of this. Assume that a quantity $q_0 = a + \sqrt{b}$ is a zero of a chromatic polynomial $P(G, q)$ of a graph G and assume that a is rational and $b > 0$ is rational but is not a perfect square, so q_0 is irrational. Then since the coefficients of all terms in $P(G, q)$ are rational (indeed, are integers), it must be the case that the algebraic conjugate, $a - \sqrt{b}$ is also a zero of $P(G, q)$ so that the product $[q - (a + \sqrt{b})][q - (a - \sqrt{b})] = q^2 - 2aq + (a^2 - b)$ involves rational coefficients. For $q = B_5$, this would imply that $(1/2)(3 - \sqrt{5}) = 0.381966$ is a chromatic zero. However, this is not possible because of the theorem [57, 100] that the interval $q \in (0, 1)$ is free of chromatic zeros.

Although the Hanoi fractal H_∞ is a self-similar object rather than a regular lattice, its effective vertex degree is $\Delta_{\text{eff}} = 3$. A comparison with q_c values for regular lattices with

various vertex degrees Δ or effective vertex degrees Δ_{eff} is thus of interest. The value that we infer for $q_c(H_\infty)$ is equal to the value $q_c(hc) = (1/2)(3 + \sqrt{5})$ for the honeycomb lattice, which has $\Delta = 3$ (see, e.g., [103, 104]). However, it should be cautioned that the infinite- n limits of two families of n -vertex graphs with the same Δ may have different values of q_c . Consider, for example, strips of the square lattice with length L_x vertices, transverse width L_y vertices, and toroidal boundary conditions (i.e., periodic in the longitudinal and transverse directions). These strips are all Δ -regular graphs for any L_x and L_y . But in the infinite-length limits $L_x \rightarrow \infty$ with fixed width L_y , the $L_y = 2$ strip of the square lattice has $q_c = 2$ [58], the $L_y = 3$ strip has $q_c = 3$ [81], and the $L_y = 4$ strip has $q_c = 2.7827657$ [89]. (The $L_y = 2$ toroidal strip of the square lattice has double transverse edges, and could be removed from this comparison by stipulating that families of graphs to be used for the q_c comparison in the respective $n \rightarrow \infty$ limits must not have multiple edges, but this still leaves the $L_y = 3$ and $L_y = 4$ toroidal square-lattice strips, which have no multiple edges, the same Δ value of 4, and different values of q_c .) Furthermore, infinite- n limits of n -vertex families of graphs with different Δ values can have the same q_c . Some examples are provided by the comparison of the $n \rightarrow \infty$ limit of the circuit graph C_n , which has $\Delta = 2$ and $q_c = 2$, and the $L_x \rightarrow \infty$ limit of a $L_x \times L_y$ strip of the square lattice with periodic longitudinal (L_x) and free transverse (L_y) boundary conditions, which has $\Delta = 3$ and $q_c = 2$. Another example is the $L_x \rightarrow \infty$ limit of the homeomorphic expansion of the $L_y = 2$ cyclic strip of the square lattice with s additional vertices added to each horizontal edge, which has Δ_{eff} ranging between 3 for $s = 0$ and 2 for $s \gg 1$, but which has $q_c = 2$ for all s [77]. Nonetheless, it is of interest that the $q_c(H_\infty)$ value that we infer for the Hanoi fractal is equal to $q_c(hc)$, and $\Delta_{\text{eff}}(H_\infty) = 3$, equal to $\Delta(hc) = 3$ for the honeycomb lattice.

These patterns of chromatic zeros for the m 'th iterate Hanoi graphs are similar to the patterns that we found for the corresponding m 'th iterates of the Sierpinski graphs in [23], with one difference being our inferred $q_c(H_\infty) = (1/2)(3 + \sqrt{5})$, while our inferred value of q_c for S_∞ in [23] was $q_c(S_\infty) = 3$. A notable aspect of the patterns of zeros of these chromatic polynomials $P(H_m, q)$ is the absence of complex-conjugate pairs of zeros extending into the interior of the region inside of the outer approximate envelope of zeros. This is in contrast to our results for chromatic zeros of Sierpinski iterates S_m displayed in Figs. 1 and 2 of Ref. [23], where we showed the zeros of $P(S_4, q)$ and $P(S_5, q)$. As is evident, e.g., in Fig. 2 of Ref. [23], there is a smaller oval-like ring of zeros crossing the real axis at $q \simeq 2.6$ and $q \simeq 2.74$, and thus located inward of the rightmost part of the outer envelope of zeros. The pattern of zeros for $P(H_m, q)$ that we find also contrasts with the results that we obtained with R. Roeder in [29] for the chromatic zeros of the m 'th iterates of the Diamond Hierarchical Lattices, D_m , including rigorous results for the accumulation locus of zeros \mathcal{B}_q in the $m \rightarrow \infty$

limit. To the left of the crossing of \mathcal{B}_q at $q_c(D_\infty) = 3$, there are an infinite number of zero-free regions and associated intervals on the real axis separated from each other by crossings of \mathcal{B}_q , starting with a zero-free region containing the real interval extending from $q = 3$ downward to a crossing of \mathcal{B}_q at

$$q = -\frac{1}{3}(1 + 3\sqrt{57})^{1/3} + \frac{8}{3(1 + 3\sqrt{57})^{1/3}} + \frac{5}{3} \simeq 1.638897, \quad (5.8)$$

then another zero-free region containing the real interval $q \in (1.409700, 1.638897)$, another crossing at 1.409700, and so forth. This infinite series of progressively smaller zero-free regions, associated zero-free real interval, and crossing points approach the point $q = 32/27$ from above. (See Table II in [29] for a list of the first 10 crossing points.) As is evident from the explicit zeros shown in Fig. 3 of [29], there is an indication of the first two of these infinitely many zero-free intervals and crossing points from the zeros of $P(D_4, q)$. A similar indication is visible in Fig. 1 of [23] showing the zeros of $P(S_4, q)$.

A triangulation is a graph all of whose faces are triangles. Although the initial Hanoi graph, H_0 , is a triangle, the H_m with $m \geq 1$ are not triangulations. For example, H_1 contains three triangular faces (c.f. Eq. (2.18)) and one 6-sided face; H_2 contains nine triangular faces, three 6-sided faces, and one 12-sided face, and so forth for higher m . As stated in Eq. (2.19), in the limit $m \rightarrow \infty$, $2/3$ of the faces are triangles. Given that triangles comprise a majority of the faces in this limit, it is of interest to investigate how strong is the deviation from the Tutte upper bound for triangulation graphs. This bound is as follows [105]: If G is a (planar) triangulation, denoted G_t , then

$$|P(G_t, \phi + 1)| \leq (\phi - 1)^{n(G_t)-5}, \quad \text{i.e.,} \quad |P(G_t, B_5)| \leq (B_5 - 2)^{n(G_t)-5}. \quad (5.9)$$

Since $B_5 - 2 = 0.6180\dots < 1$, this upper bound decreases exponentially rapidly as a function of $n(G_t)$. The Tutte upper bound (5.9) is sharp, since it is saturated for the simplest triangulation, namely a triangle graph, K_3 . For K_3 , the bound is that $|P(K_3, B_5)| \leq (B_5 - 2)^{-2} = B_5$, and $P(K_3, B_5) = B_5$. For graphs that are not triangulations, as well as graphs for which a majority of the faces are triangles, it is of interest to determine how close they come to saturating the Tutte upper bound. For this purpose, one defines the ratio [106, 107].

$$r(G) = \frac{|P(G, B_5)|}{(B_5 - 2)^{n(G)-5}}. \quad (5.10)$$

The bound (5.9) is thus the statement that if G is a triangulation, G_t , then $r(G_t) \leq 1$. We find that for $m \geq 2$ where H_m is not a triangulation, the ratio $r(H_m)$ is considerably larger than 1.

VI. ZEROS OF $Z(H_m, q, v)$ IN THE q PLANE AT FINITE TEMPERATURE

As stated in Eq. (2.2), for an arbitrary graph G , the chromatic polynomial $P(G, q)$ is equal to the partition function of the zero-temperature Potts antiferromagnet, $Z(G, q, v = -1)$. As the temperature T increases from 0 to ∞ for the Potts antiferromagnet, v increases from -1 to 0^- . In Fig. 5 we show a plot of zeros of $Z(H_4, q, v)$ in the q plane for $v = -0.5$, an illustrative finite-temperature value of v for the Potts antiferromagnet. The pattern of zeros is smoother than for $v = -1$, and it is contracting toward $q = 0$. As $v \rightarrow 0^-$, the zeros all move in toward $q = 0$, in accord with the general property that for an arbitrary graph G , if $v = 0$, then $Z(G, q, v = 0) = q^{n(G)}$, so that all of the zeros occur at $q = 0$.

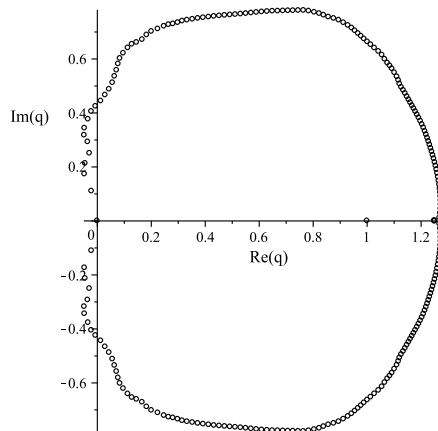


FIG. 5. Zeros of the Potts partition function $Z(H_4, q, v)$ in the q plane for $v = -0.5$.

As T decreases from ∞ through finite values for the Potts ferromagnet, v increases from 0 through positive values. In Fig. 6 we show a plot of the zeros of $Z(H_4, q, v)$ in the q plane for a representative finite-temperature value of v for the Potts ferromagnet, namely $v = 0.5$. In this case, the zeros again exhibit a roughly oval form, and, aside from the zero at $q = 0$, most of them have negative real parts (some zeros with nonzero imaginary parts have small positive real parts).

VII. ZEROS OF $Z(H_m, q, y)$ IN THE y PLANE

It is also of interest to investigate the zeros of $Z(H_m, q, v)$ in the complex plane of the temperature-dependent Boltzmann variable v , and we have carried out this study. For

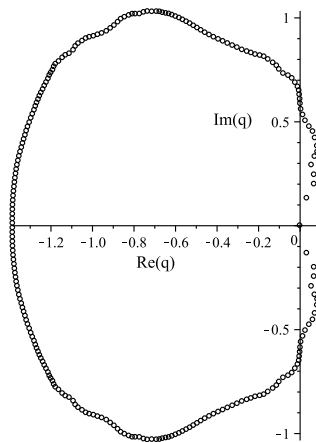


FIG. 6. Zeros of the Potts partition function $Z(H_4, q, v)$ in the q plane for $v = 0.5$.

convenience, we will plot these zeros in the plane of the variable $y = v + 1 = e^K$ and will use the notation

$$Z(G, q, y) \equiv Z(G, q, v)_{v=y-1} . \quad (7.1)$$

As a historical note, it may be recalled that zeros of partition functions of spin models on regular lattices have long been of interest, dating from the pioneering analyses by Lee and Yang [108, 109] of zeros of the Ising model in the plane of a Boltzmann variable $z = e^{\beta H}$, where H is an external magnetic field, and an analysis by Fisher of zeros of the partition function of the Ising model (in zero external magnetic field) in a temperature-dependent Boltzmann variable [110]. It was shown in early work [6]-[9] that a necessary condition for a discrete spin model on the $m \rightarrow \infty$ limit of a hierarchical family of graphs G_m to have an order-disorder phase transition at finite temperature is that in this limit, the resultant fractal has vertices with an infinite ramification number, R . Here, as defined in [6]-[9], the ramification number R of a given vertex in a hierarchical graph G_m is the number of edges that must be cut to isolate the vertex from the rest of the graph. (Different vertices may have different ramification numbers.) It was noted in [6, 8] that the R numbers for vertices in the Sierpinski gasket fractal are finite, and therefore the Potts model (with either sign of J) does not have a physical finite-temperature phase transition on S_∞ . The same property holds for Hanoi graphs, and hence the Potts model with either sign of J does not have a finite-temperature order-disorder transition on the H_∞ fractal. Consequently, the accumulation locus \mathcal{B}_y cannot cross the positive y plane at any finite value of y .

In Figs. 7-10 we show zeros of $Z(H_4, q, y)$ in the y plane for $q = 2, B_5, 3, 5$. For each figure, the number of zeros, counting multiplicity, is equal to the degree of $Z(H_m, q, y)$ in y ,

namely $\deg_y[Z(H_m, q, y)] = e(H_m)$, as given in Eq. (2.15). A remark is in order concerning the plot of zeros of $Z(H_4, q = 2, y)$ in Fig. 7. For this $q = 2$ case, we find that $Z(H_m, q = 2, y)$ has multiple zeros at $y = 0$ and $y = -1$. For the cases that we have calculated with $m \geq 1$, $Z(H_m, q = 2, y)$ has a general form involving the factor y^{3^m} and, for $m \geq 1$, the factor $(y + 1)^{(3/2)(3^m - 1)}$, as well as possible other repeated factors such as powers of $(y^2 - y + 2)$. As illustrative examples with $0 \leq m \leq 2$, we display

$$Z(H_0, q = 2, y) = 2y(y^2 + 3) \quad (7.2)$$

$$Z(H_1, q = 2, y) = 2y^3(y + 1)^3(y^2 - y + 2)(y^4 - 2y^3 + 8y^2 + 2y + 7) \quad (7.3)$$

and

$$\begin{aligned} Z(H_2, q = 2, y) &= 2y^9(y + 1)^{12}(y^2 - y + 2)^3(y^4 - 3y^3 + 7y^2 - y + 4) \\ &\times \left(y^8 - 6y^7 + 26y^6 - 38y^5 + 84y^4 - 2y^3 + 102y^2 + 46y + 43 \right) \end{aligned} \quad (7.4)$$

The factor of y^{3^m} in $Z(H_m, q = 2, y)$ is the same as for $Z(S_m, q = 2, y)$ and reflects the fact that as $y \rightarrow 0$, i.e., $v \rightarrow -1$, $Z(H_m, q, y) \rightarrow P(H_m, q)$, but $P(H_m, 2) = 0$ because it is not possible to perform a proper vertex coloring of H_m with just 2 colors. Owing to these multiple zeros, the number of separate zeros in Fig. 7 is less than the total number of zeros, $e(H_4) = 363$. It is worthwhile observing here how, in the two-variable polynomial $Z(H_m, q, y)$, one can see the approach to the zero at $Z(H_m, q = 2, y = 0)$ by setting $q = 2$ and noting the presence of the factor $y^{3^m} = (v + 1)^{3^m}$ in $Z(H_m, q = 2, y)$ or by setting $y = 0$ and noting the presence of the factor $(q - 2)^{3^m}$ in $Z(H_m, q, y = 0) = P(H_m, q)$ (recall Eq. (3.1)).

If, for the Potts antiferromagnet, the asymptotic locus of chromatic zeros $\mathcal{B}_q(y = 0)$ crosses the real- q axis at a maximal point q_c , this connotes a zero-temperature critical point, so that the corresponding asymptotic locus of Fisher zeros, \mathcal{B}_y , should cross the real y axis at $y = 0$. Indeed, if one views this locus as an algebraic variety in the \mathbb{C}^2 space of (q, y) , this singular behavior occurs at a given point, $(q, y) = (q_c, 0)$, and one is observing “slices” through this algebraic variety with one or the other variable held fixed in these crossings. For example, the property that $q_c = 3$ for the infinite square lattice [37, 38] and also for infinite-length, finite-width square-lattice strips with self-dual boundary conditions [90, 91], correspond to the $T = 0$ critical point of the $q = 3$ Potts antiferromagnet on these lattices. Similarly, the property that $q_c(\text{tri}) = 4$ for the triangular lattice [68, 69] corresponds to the $T = 0$ critical point of the PAF on this lattice, and these results are in agreement with studies of Fisher zeros on finite sections of these lattices, e.g., [103, 104, 111]. Among fractals, $q_c = 3$

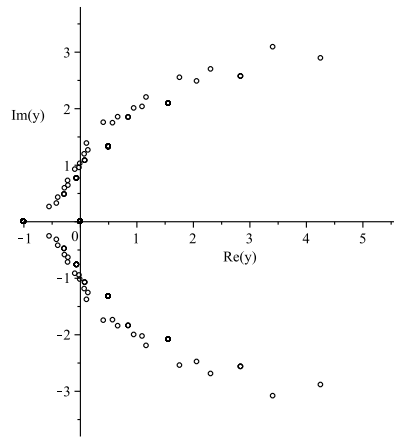


FIG. 7. Zeros of $Z(H_4, q, y)$ in the y plane for $q = 2$.

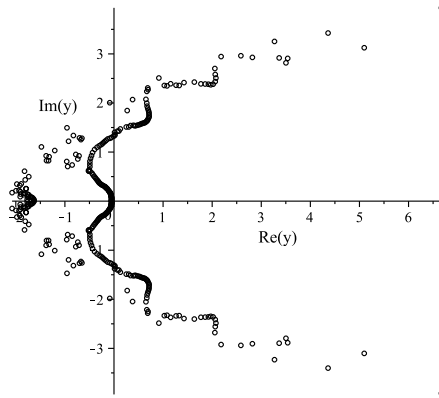


FIG. 8. Zeros of $Z(H_4, q, y)$ in the y plane for $q = (1/2)(3 + \sqrt{5})$.

for the Diamond Hierarchical Lattice D_∞ , and this was shown to correspond to a $T = 0$ critical point of the PAF on D_∞ [29]. Thus, a consistency check on our inferred value of $q_c(H_\infty)$ in Eq. (5.1) is to calculate Fisher zeros of $Z(H_m, q, y)$ for $q = B_5$ and confirm that these are consistent with the property that the asymptotic locus \mathcal{B}_y passes through $y = 0$. We have performed this check and show, as an example, the zeros of $Z(H_4, q = B_5, y)$ in Fig. 8. As is evident in this figure, even at the moderate iteration stage $m = 4$, these zeros pass very close to $y = 0$, and are fully in accord with the inference that as $m \rightarrow \infty$, the locus \mathcal{B}_y for $q = B_5$ would pass through this point $y = 0$. Parenthetically, we note that these zeros

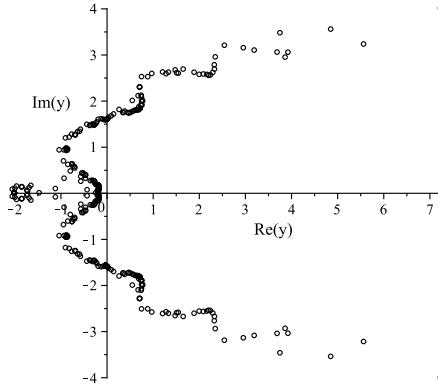


FIG. 9. Zeros of $Z(H_4, q, y)$ in the y plane for $q = 3$.

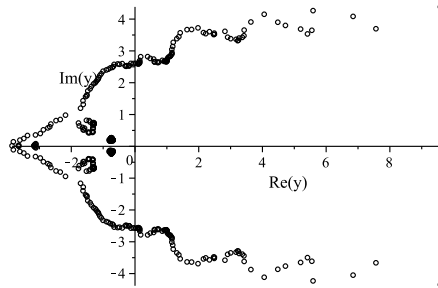


FIG. 10. Zeros of $Z(H_4, q, v)$ in the y plane for $q = 5$.

in the y plane for $q = B_5$ and $q = 5$ (as well as larger q , such as in Fig. 11 below) exhibit an intriguing wavy structure as well as concentrations at (unphysical) points and regions in the third and fourth quadrants.

VIII. LARGE- q BEHAVIOR OF ZEROS OF $Z(H_m, q, y)$ IN THE y PLANE

One interesting result concerns the zeros in the large- q limit. For regular (non-fractal) lattices, these have previously been studied, e.g., in [112] and, by us, in [113]. In the

thermodynamic limit for $d \geq 2$ on these regular lattices, the Potts ferromagnet has a finite-temperature phase transition, so that \mathcal{B}_y crosses the positive y axis. In contrast, as was mentioned above, since the Potts model has no order-disorder phase transition at any finite temperature on the H_∞ fractal, the locus \mathcal{B}_y does not cross the positive y axis at any point. This is the analogue, for Hanoi graphs, of the feature that we mentioned for Sierpinski gasket graphs in [23], that \mathcal{B}_y cannot cross the positive y axis for S_∞ . We recall, however, that the Diamond Hierarchical Lattice has infinite ramification number, as does the Sierpinski carpet [9], so that, as was discussed in [13] and more recently in [29], \mathcal{B}_y does cross the positive real y axis for the DHL fractal D_∞ .

In Figs. 11-15 we show plots of zeros of $Z(H_4, q, y)$ in the y plane for $q = 10, 10^2, 10^3, 10^4$, and 10^5 . We find that, in contrast with the sections of regular lattices that were studied in Refs. [112, 113], where the y -plane zeros in the large- q limit approach an approximately circular form with $|y| \simeq q^{2/\Delta}$, here we find a different type of behavior, namely that, for $q \gg 1$, the zeros cluster approximately along, or near to, parts of the edges of an equilateral triangle with vertices at points that scale like $y_j \sim q^{2/3} e^{\pm \frac{2\pi i}{3}}$, where $j = 0, 1, 2$, or equivalently,

$$v_1 \sim q^{2/3}, \quad v_{2,3} \sim q^{2/3} e^{\pm \frac{2\pi i}{3}}. \quad (8.1)$$

These are equivalent because the magnitudes of these zeros grow like $|q|^{2/3}$ in the large- q limit, and hence there is a negligibly small difference between the positions of the zeros in the y plane and the $v = y - 1$ plane. However, the zeros avoid the regions around the three apex points of this triangle; in particular, they avoid the apex point on the positive y axis, as noted above.

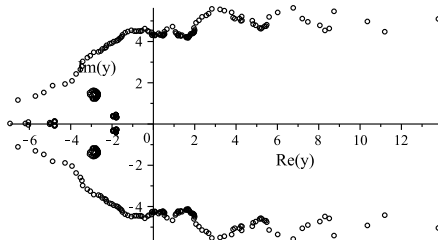


FIG. 11. Zeros of $Z(H_4, q, y)$ in the y plane for $q = 10$.

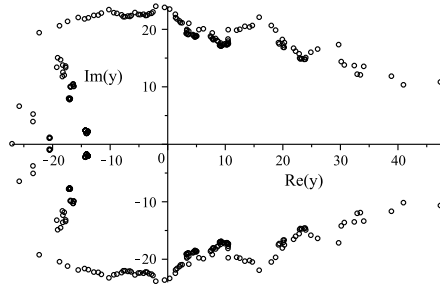


FIG. 12. Zeros of $Z(H_4, q, y)$ in the y plane for $q = 10^2$.

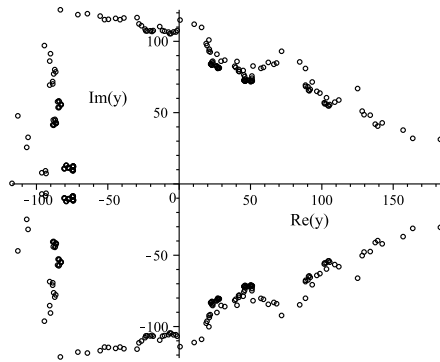


FIG. 13. Zeros of $Z(H_4, q, y)$ in the y plane for $q = 10^3$.

It is also instructive to display these zeros as a function of a variable

$$\xi = \frac{v}{q^{2/3}}, \quad (8.2)$$

which, up to negligibly small terms in the large- q limit, is equivalent to $\xi = y/q^{2/3}$. We show these plots for $q = 10^4$ and $q = 10^5$ in Figs. 16 and 17. The apex points in this ξ plane have magnitudes $|\xi| \simeq 2$. An important property of these zeros is invariance under the action of a multiplicative \mathbb{Z}_3 group with the elements

$$\mathbb{Z}_3 : \quad \{1, e^{2\pi i/3}, e^{4\pi i/3}\}, \quad (8.3)$$

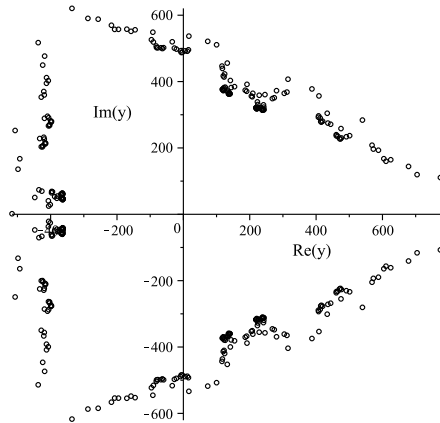


FIG. 14. Zeros of $Z(H_4, q, y)$ in the y plane for $q = 10^4$.

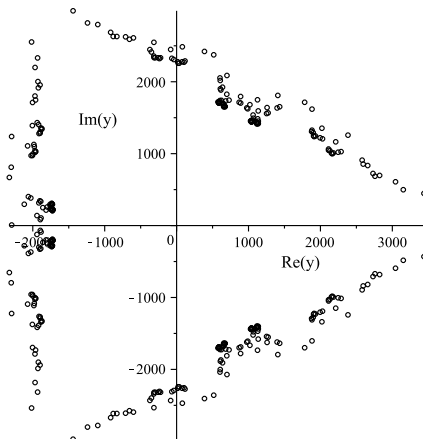


FIG. 15. Zeros of $Z(H_4, q, y)$ in the y plane for $q = 10^5$.

including rotations in the complex ξ plane by an angle of $\pm 2\pi/3$ radians.

We provide some insight into this behavior as follows. We will show that in the limit $q \rightarrow \infty$, the zeros of $Z(H_m, q, v)$ are determined by a polynomial in the variable

$$\eta = \xi^3 = \frac{v^3}{q^2}. \quad (8.4)$$

This also explains why, for a given large q , the zeros in the v plane or equivalently, the ξ plane, are invariant under the action of the elements of the \mathbb{Z}_3 group (8.3). Consider, for example, $Z(H_1, q, v)$, the expression for which is given in Eq. (A6) in Appendix A. Expressing this in

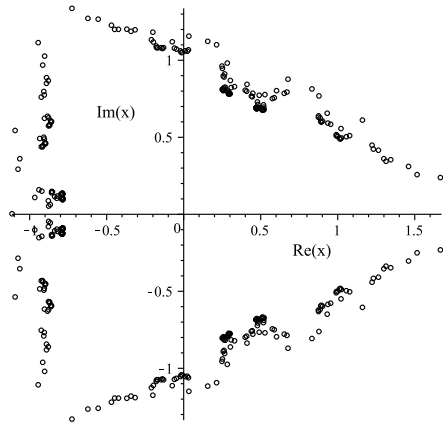


FIG. 16. Zeros of $Z(H_4, q, y)$ in the $\xi = v/q^{2/3}$ plane for $q = 10^4$.

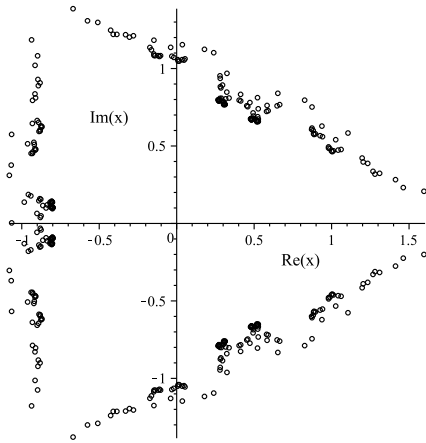


FIG. 17. Zeros of $Z(H_4, q, y)$ in the $\xi = v/q^{2/3}$ plane for $q = 10^5$.

terms of ξ and expanding as $q \rightarrow \infty$, we get

$$\begin{aligned}
 Z(H_1, q, v) &= q^9 \left[\left(\xi^{12} + \xi^9 + 3\xi^6 + 3\xi^3 + 1 \right) \right. \\
 &\quad + \frac{3}{q^{1/3}} \left(2\xi^{10} + 6\xi^7 + 9\xi^4 + 4\xi \right) \\
 &\quad \left. + \frac{6}{q^{2/3}} \left(2\xi^{11} + 8\xi^8 + 18\xi^5 + 11\xi^2 \right) \right]
 \end{aligned}$$

$$+ \frac{1}{q} \left(75\xi^9 + 247\xi^6 + 217\xi^3 \right) + O\left(\frac{1}{q^{4/3}}\right) \Big], \quad (8.5)$$

where the additional terms are polynomials in ξ multiplied by negative powers $q^{-4/3}$, $q^{-5/3}$, q^{-2} , etc. Recalling Eq. (2.14), this example shows in the limit $q \rightarrow \infty$,

$$\lim_{q \rightarrow \infty} \frac{Z(H_1, q, v)}{q^{n(H_1)}} = \Omega(H_1, \eta) \quad (8.6)$$

where

$$\Omega(H_1, \eta) = \eta^4 + \eta^3 + 3\eta^2 + 3\eta + 1. \quad (8.7)$$

This method generalizes to higher m , which shows that

$$\lim_{q \rightarrow \infty} \frac{Z(H_m, q, v)}{q^{n(H_m)}} = \Omega(H_m, \eta) \quad (8.8)$$

where $n(H_m) = 3^{m+1}$ was given in Eq. (2.14) and $\Omega(H_m, \eta)$ is a polynomial in η . For example, for the next higher iterate, H_2 , we calculate

$$\begin{aligned} \Omega(H_2) &= (\eta + 1)(\eta^{12} + 3\eta^{10} + 9\eta^9 + 19\eta^8 + 38\eta^7 + 58\eta^6 \\ &+ 71\eta^5 + 73\eta^4 + 56\eta^3 + 28\eta^2 + 8\eta + 1). \end{aligned} \quad (8.9)$$

Because, in the limit $q \rightarrow \infty$, $Z(H_m, q, v)$ reduces to the prefactor $q^{n(H_m)}$ times a function of ξ^3 and thus of v^3 , this shows that the zeros of $Z(H_m, q, v)$ in this limit are invariant under the elements of the \mathbb{Z}_3 group (8.3) in the ξ plane, and equivalently, in the v and y planes. The property that these zeros accumulate approximately along parts of the edges of the equilateral triangle with apex points (8.1) depends on further details of $Z(H_m, q, v)$.

It is useful to contrast these findings with the results that we obtained in Ref. [113]. In that work we discussed the analytic basis that is responsible for the approach of the Potts partition function zeros in the complex plane of the variable $\xi = v/q^{2/\Delta}$ to the circle $|\xi| = 1$, as $q \rightarrow \infty$, for regular lattices with vertex degree Δ (or Δ_{eff}). This circular locus of the accumulation set of zeros in the ξ plane is invariant under the full rotation group $U(1) \approx O(2)$. We also showed this behavior for the Sierpinski iterates in [23] and for the DHL iterates in [29] with Δ_{eff} . In addition to our derivation given above, an explanation for why the zeros do not cluster on or near to this circle is provided by our analysis in [113]. There we noted that our derivation only applied to lattice graphs with the property that deleting several edges would not lead to the appearance of disconnected graphical components. As stated in [113], this condition is satisfied for sufficiently large sections of lattice graphs with finite aspect ratios L_i/L_j , where L_i and L_j denote lengths along two different lattice directions. As

we remarked in [23, 29], this condition is also true for the Sierpinski gasket iterates S_m and the DHL iterates D_m . However, in contrast, it is not true for the Hanoi iterates H_m ; if one deletes any two of the edges on the middle exterior sides of the outer triangular boundary, this separates the previously connected graph H_m into two disjoint components. Our detailed analysis above shows that the symmetry of the zeros in the ξ plane in the $q \rightarrow \infty$ limit for H_m graphs is the finite subgroup \mathbb{Z}_3 of the full rotation group $U(1)$.

IX. CONCLUSIONS

In summary, in this work we have investigated properties of the Potts model partition function $Z(H_m, q, v)$ on m 'th iterate Hanoi graphs and have used the results to draw inferences about the $m \rightarrow \infty$ limit. We have calculated the ground state degeneracy per vertex of the Potts antiferromagnet on H_m for $q = 3$ and $q = 4$ and a large range of m and have used the results to infer estimates of $W(H_\infty, q)$ for these values of q . The values were compared with the corresponding ground state degeneracy for the Potts antiferromagnet on other lattices. Further, we have presented calculations of zeros of $P(H_m, q)$ for m up to 4, and from these we have inferred that in the $m \rightarrow \infty$ limit, the asymptotic accumulation locus of chromatic zeros, \mathcal{B}_q for $v = y - 1 = -1$, crosses the real q axis at $q_c(H_\infty) = B_5 = (1/2)(3 + \sqrt{5})$. This means that the Potts antiferromagnet with $q = B_5$ has a zero-temperature critical point on the H_∞ fractal. We have obtained further evidence in support of this inference by calculating the partition function zeros in the y plane for this value of q and showing that they are consistent with the inference that the locus of zeros in the limit $m \rightarrow \infty$ passes through the $T = 0$ point for the antiferromagnetic Potts model, at $y = 0$. Results were also given for the zeros of the partition function on H_m (i) in the q plane for the Potts antiferromagnet and ferromagnet at illustrative finite temperatures and (ii) in the y plane for several values of q in addition to B_5 . Finally, we have computed the zeros in the y plane for $q \gg 1$ and have shown that they aggregate approximately along parts of the sides of the triangle whose apex points scale like $q^{2/3}$ and $q^{2/3}e^{\pm 2\pi i/3}$, exhibiting an invariance under elements of the multiplicative \mathbb{Z}_3 group. Some comparisons were made with our earlier work on the related Sierpinski fractal.

ACKNOWLEDGMENTS

The research of S.-C.C. was supported in part by the Taiwan Ministry of Science and Technology (MOST) grant MOST 111-2115-M-006-012-MY2 and the Taiwan National Sci-

ence and Technology Council (NSTC) grant NSTC 113-2115-M-006-006-MY2. The research of R.S. was supported in part by the U.S. National Science Foundation Grant NSF-22-10533.

Appendix A: Iterative Procedure for Calculation of $T(H_m, x, y)$

For reference, here we remark on the nonlinear iterative procedure derived in [24] for calculating the Tutte polynomial $T(H_m, x, y)$. (Ref. [24] used a different labelling convention for the Hanoi graphs, according to which $H_{m'}$ in [24] is H_{m+1} in the labelling convention used here, so $m' = m + 1$.) This procedure expresses $T(H_m, x, y)$ in terms of a sum of three auxiliary functions $F_{0,m}(x, y)$, $F_{1,m}(x, y)$, and $F_{2,m}(x, y)$, which satisfy nonlinear recursive relations with lower-order auxiliary functions. Explicitly (suppressing the arguments in $F_{s,m} \equiv F_{s,m}(x, y)$, $s = 0, 1, 2$),

$$T(H_m, x, y) = F_{2,m} + 3F_{1,m} + F_{0,m} \quad (\text{A1})$$

where

$$\begin{aligned} F_{2,m+1} &= (y-1)F_{2,m}^3 + 3(x-1)^{-1}F_{2,m}F_{1,m}(2F_{2,m} + F_{1,m}) \\ &+ 3F_{2,m}(F_{2,m} + F_{1,m})^2 \end{aligned} \quad (\text{A2})$$

and

$$\begin{aligned} F_{1,m+1} &= (y-1)F_{2,m}^2F_{1,m} \\ &+ (x-1)^{-1}\left(F_{2,m}^2F_{0,m} + 7F_{2,m}F_{1,m}^2 + 2F_{2,m}F_{1,m}F_{0,m} + 4F_{1,m}^3 + F_{1,m}^2F_{0,m}\right) \\ &+ 7F_{2,m}^2F_{1,m} + 2F_{2,m}^2F_{0,m} + 14F_{2,m}F_{1,m}^2 + 4F_{2,m}F_{1,m}F_{0,m} + 7F_{1,m}^3 + 2F_{1,m}^2F_{0,m} \\ &+ (x-1)\left(F_{2,m}^3 + 5F_{2,m}^2F_{1,m} + F_{2,m}^2F_{0,m} + 7F_{2,m}F_{1,m}^2 + 2F_{2,m}F_{1,m}F_{0,m}\right. \\ &\left.+ 3F_{1,m}^3 + F_{1,m}^2F_{0,m}\right) \end{aligned} \quad (\text{A3})$$

with the initial values

$$F_{2,0} = y + 2, \quad F_{1,0} = x - 1, \quad F_{0,0} = (x - 1)^2. \quad (\text{A4})$$

Since these expressions are nonsingular at $x = 1$, the presence of the factors $(x-1)^{-1}$ implies certain identities. For example, in Eq. (A2), the quantity $F_{2,m}F_{1,m}(2F_{2,m} + F_{1,m}) = 0$ at

$x = 1$, and similarly with the quantity multiplying the factor of $(x - 1)^{-1}$ in Eq. (A3). The recursion relation for $F_{0,m+1}$ is longer, and we refer the reader to (Theorem 4.3 of) Ref. [24] for it. From the Tutte polynomial one can calculate the Potts model partition function via the relation (2.9) with (2.10) and (2.11). For our work we have calculated $T(H_m, x, y)$ with m to 4 inclusive. As an illustration, we list $T(H_1, x, y)$:

$$\begin{aligned}
T(H_1, x, y) &= x^8 + 4x^7 + 3x^6y + 7x^6 + 9x^5y + 3x^4y^2 + 8x^5 + 12x^4y \\
&+ 6x^3y^2 + x^2y^3 + 8x^4 + 13x^3y + 9x^2y^2 + 4xy^3 + y^4 + 7x^3 + 12x^2y \\
&+ 9xy^2 + 3y^3 + 4x^2 + 6xy + 3y^2 + x + y .
\end{aligned} \tag{A5}$$

The corresponding expression for $Z(H_1, q, v)$ is

$$\begin{aligned}
Z(H_1, q, v) &= q \left[v^{12} + 12v^{11} + 6v^{10}q + v^9q^2 + 60v^{10} + 75v^9q + 48v^8q^2 \right. \\
&+ 18v^7q^3 + 3v^6q^4 + 144v^9 + 312v^8q + 351v^7q^2 + 247v^6q^3 \\
&+ 108v^5q^4 + 27v^4q^5 + 3v^3q^6 + 135v^8 + 423v^7q + 674v^6q^2 \\
&\left. + 684v^5q^3 + 468v^4q^4 + 217v^3q^5 + 66v^2q^6 + 12vq^7 + q^8 \right] .
\end{aligned} \tag{A6}$$

The expressions for $T(H_m, x, y)$ and $Z(H_m, q, v)$ become quite lengthy for higher m , so we do not list these explicitly here. For example, while $T(H_1, x, y)$ and $Z(H_1, q, v)$ have 24 and 25 terms, respectively, as displayed in Eqs. (A5) and (A6), $T(H_2, x, y)$ and $Z(H_2, q, v)$ have 195 and 196 terms, respectively, and so forth for higher m .

Appendix B: Sierpinski Gasket Graphs

In this Appendix we list some properties of m 'th iterates of Sierpinski gasket graphs, S_m . Our labelling convention for the S_m is the same as we used in [23] and [42]-[49]. (This also maintains uniformity with our labelling convention for the H_m , so that both H_0 and S_0 are the same graph, namely $K_3 = C_3$.)

The number of vertices in the m 'th iterate Sierpinski graph, $n(S_m)$, is

$$n(S_m) = \frac{3(3^m + 1)}{2} , \tag{B1}$$

and the numbers of edges, $e(S_m)$, is

$$e(S_m) = 3^{m+1} . \quad (\text{B2})$$

In comparison with the Hanoi iterates, we thus have

$$\lim_{m \rightarrow \infty} \frac{n(H_m)}{n(S_m)} = 2 \quad (\text{B3})$$

and

$$\lim_{m \rightarrow \infty} \frac{e(H_m)}{e(S_m)} = \frac{3}{2} . \quad (\text{B4})$$

The cyclomatic number of S_m is thus

$$c(S_m) = \frac{3^{m+1} - 1}{2} . \quad (\text{B5})$$

The effective vertex degree of S_∞ is

$$\Delta_{\text{eff}}(S_\infty) = 4 . \quad (\text{B6})$$

The number of faces in S_m , denoted $N_F(S_m)$, is

$$N_F(S_m) = \frac{3^{m+1} - 1}{2} , \quad (\text{B7})$$

which is equal to $c(S_m)$. The number of triangles in S_m , denoted $N_t(S_m)$, is given by the coefficient of the term z^m in the Taylor series expansion of the function $(1+z)/(1-3z)$ about $z=0$, i.e.,

$$\begin{aligned} \frac{1+z}{1-3z} &= \sum_{j=0}^{\infty} N_t(S_j) z^j = 1 + 4z + 12z^2 + 36z^3 + 108z^4 \\ &+ 324z^5 + 972z^6 + 2916z^7 + 8748z^8 + \dots \end{aligned} \quad (\text{B8})$$

Therefore, in the limit $m \rightarrow \infty$, the ratio of triangular faces to the total number of faces in S_m is

$$\lim_{m \rightarrow \infty} \frac{N_t(S_m)}{N_F(S_m)} = \frac{8}{9} . \quad (\text{B9})$$

This is evidently slightly higher than the value of $2/3$ for the corresponding ratio for Hanoi graphs.

The Tutte polynomial for $m=0$ is elementary: $T(S_0, x, y) = T(K_3, x, y) = x^2 + x + y$. For $m=1$,

$$T(S_1, x, y) = x^5 + 4x^4 + 4x^3y + 3x^2y^2 + 3xy^3 + y^4 + 6x^3 + 9x^2y + 6xy^2$$

$$+ 2y^3 + 4x^2 + 6xy + 3y^2 + x + y \quad (\text{B10})$$

This yields

$$P(S_1, q) = q(q-1)(q-2)^4. \quad (\text{B11})$$

As we calculated for the work in [23],

$$\begin{aligned} P(S_2, q) = & q(q-1)(q-2)^6 \left(q^7 - 14q^6 + 85q^5 - 292q^4 + 620q^3 \right. \\ & \left. - 831q^2 + 676q - 272 \right). \end{aligned} \quad (\text{B12})$$

and

$$\begin{aligned} P(S_3, q) = & q(q-1)(q-2)^9 \left(q^{31} - 62q^{30} + 1864q^{29} - 36200q^{28} \right. \\ & + 510406q^{27} - 5567417q^{26} + 48885472q^{25} - 354996791q^{24} \\ & + 2173710199q^{23} - 11385918177q^{22} + 51580729311q^{21} \\ & - 203815546118q^{20} + 707080076667q^{19} - 2164599135972q^{18} \\ & + 5869749718724q^{17} - 14137926421037q^{16} + 30300472680589q^{15} \\ & - 57835231423884q^{14} + 98313224299548q^{13} - 148699316658336q^{12} \\ & + 199737162065052q^{11} - 237551626238256q^{10} + 249080624015424q^9 \\ & - 228900210474672q^8 + 182904284767200q^7 - 125717659569984q^6 \\ & + 73230886710720q^5 - 35383634429696q^4 + 13722399529984q^3 \\ & \left. - 4041086324736q^2 + 811162107904q - 84017414144 \right). \end{aligned} \quad (\text{B13})$$

In [23] we calculated $P(S_m, q)$ for higher m , but the expressions were too lengthy to give there.

With the notation of Eq. (7.1), for the cases that we calculated, we find that $Z(S_m, 2, y)$ has the factors y^{3^m} and, for $m \geq 1$, $(y^2 + 1)^{3^{m-1}}$, where $y = v + 1$. The factor of y^{3^m} is the same as for $Z(H_m, 2, y)$ and reflects the property that as $y \rightarrow 0$, $Z(S_m, q, y) \rightarrow P(S_m, q)$, but

$P(S_m, 2) = 0$ because it is not possible to perform a proper vertex coloring of S_m with just 2 colors. As illustrations of the explicit expressions of $Z(S_m, 2, y)$ for the first few values of m , we note that $Z(S_0, 2, y) = Z(H_0, 2, y)$, given in Eq. (7.2), and list the following:

$$Z(S_1, 2, y) = 2y^3(y^2 + 1)(y^4 + 2y^2 + 13) \quad (\text{B14})$$

$$Z(S_2, 2, y) = 2y^9(y^2 + 1)^3(y^4 + 7)(y^8 + 26y^4 + 72y^2 + 157) \quad (\text{B15})$$

and

$$\begin{aligned} Z(S_3, 2, y) &= 2y^{27}(y^2 + 1)^9(y^4 + 7)^3(y^8 - 2y^6 + 16y^4 + 34y^2 + 79) \\ &\times \left(y^{16} - 4y^{14} + 48y^{12} + 124y^{10} + 1034y^8 + 3988y^6 + 12696y^4 + 23156y^2 + 24493 \right). \end{aligned} \quad (\text{B16})$$

-
- [1] Mandelbrot, B. B.: The Fractal Geometry of Nature. Freeman, San Francisco (1983)
 - [2] Bunde, A., Havlin, S.: Fractals and Disordered Systems. Springer, Berlin, 1991
 - [3] Pietgen, H.-O., Jürgens, J., Saupe, D.: Chaos and Fractals: New Frontiers of Science. Springer, New York (1992)
 - [4] Falconer, K.: Fractal Geometry: Mathematical Foundations and Applications. Wiley, New York (2003)
 - [5] Dhar, D.: Lattices of effectively nonintegral dimensionality. J. Math. Phys. **18**, 577-585 (1977)
 - [6] Gefen, Y., Mandelbrot, B. B., Aharony, A.: Critical phenomena on fractal lattices. Phys. Rev. Lett. **45**, 855-858 (1979)
 - [7] Gefen, Y., Aharony, A., Mandelbrot, B. B.: Phase transitions on fractals: I. Quasi-linear lattices. J. Phys. A **16**, 1267-1278 (1983)
 - [8] Gefen, Y., Aharony, A., Shapir, Y., Mandelbrot, B. B.: Phase transitions on fractals: II. Sierpinski gaskets. J. Phys. A **17**, 435-444 (1984)
 - [9] Gefen, Y., Aharony, A., Mandelbrot, B. B.: Phase transitions on fractals: III. Infinitely ramified lattices. J. Phys. A **17**, 1277-1289 (1984)

- [10] Kaufman, M., Griffiths, R. B.: Exactly solvable Ising models on hierarchical lattices. *Phys. Rev. B* **24**, 496-498 (1981)
- [11] Griffiths, R. B., Kaufman, M.: Spin systems on hierarchical lattices: Introduction and thermodynamic limit. *Phys. Rev. B* **26**, 5022-2032 (1982)
- [12] Kaufman, M., Griffiths, R.B.: Spin systems on hierarchical lattices. II. Some examples of soluble models. *Phys. Rev. B* **30**, 244-249 (1984)
- [13] Derrida, B., De Seze, L., Itzykson, C: Fractal structure of zeros in hierarchical models. *J. Stat. Phys.* **33**, 559-569 (1983)
- [14] Bhanot, G., Neuberger, H., Shapiro, J. A.: Simulation of a critical Ising fractal. *Phys. Rev. Lett.* **53** 2277-2280 (1984)
- [15] Hu, B.: Problem of universality in phase transitions on hierarchical lattices. *Phys. Rev. Lett.* **55**, 2316-2319 (1985)
- [16] Wu, Y.-K., Hu, B.: Phase transitions on complex Sierpinski carpets. *Phys. Rev. A* **35**, 1404-1411 (1987)
- [17] Hu, B., Lin, B.: Yang-Lee zeros, Julia sets, and their singularity spectra. *Phys. Rev. A* **39**, 4789-4796 (1989)
- [18] Bleher, P. M., Lyubich, M. Yu.: Julia sets and complex singularities in hierarchical Ising models. *Commun. Math. Phys.* **141**, 453-474 (1991)
- [19] Andrade, R. F. S.: Potts model on the Sierpinski gasket: A transfer matrix approach, *Phys. Rev. B* **48**, 16095-16098 (1993)
- [20] Qiao, J., Li, Y., On connectivity of Julia sets of Yang-Lee zeros. *Commun. Math. Phys.* **222**, 319—326 (2001)
- [21] Huang, M.-C., Luo, Y.-P., Liaw, T.-M.: Self-similar structure in the distribution and density of partition function zeros, *Phys. Lett. A* **320**, 180-191 (2003)
- [22] De Simoi, J.: Potts models on hierarchical lattices and renormalization group dynamics, *J. Phys. A* **42**, 095002 (2009)
- [23] Chang, S.-C., Shrock, R.: Zeros of the Potts model partition function on Sierpinski graphs, *Phys. Lett. A* **377**, 671-675 (2013)

- [24] Donno, A., Iacono, D.: The Tutte polynomial of the Sierpinski and Hanoi graphs, *Adv. in Geometry* **13**, 663-693 (2013)
- [25] Chen, H., Deng, H.: Tutte Polynomials of Scale-Free Networks, *J. Stat. Phys.* **163**, 714-732 (2016)
- [26] Bleher, A., Lyubich, M., Roeder, R. K. W.: Lee-Yang zeros for the Diamond Hierarchical Lattice and 2D rational dynamics, I. Foliation of the physical cylinder, *J. des Math. Pures et Appl.* **107**, 491-590 (2017)
- [27] Bleher, A., Lyubich, M., Roeder, R. K. W.: Lee-Yang zeros for the Diamond Hierarchical Lattice and 2D rational dynamics, II: Global pluripotential interpretation, *J. Geometric Analysis*, **30**, 777-833 (2020)
- [28] Chio, I., Roeder, R. K. W.: Chromatic zeros on hierarchical lattices and equidistribution on parameter space. *Annales de l'Institut H. Poincaré D* **8**, 49-81 (2021)
- [29] Chang, S.-C., Roeder, R. K. W., Shrock, R.: q -Plane zeros of the Potts partition function on Diamond Hierarchical Graphs. *J. Math. Phys.* **61**, 073301 (2020)
- [30] Alvarez, P. D.: Exact partition function of the Potts model on the Sierpinski gasket and the Hanoi lattice, arXiv:2306.06054v3.
- [31] Chang, S.-C., Chen, L.-C., Yang, Z.-X.: The ice model on the three-dimensional Hanoi graph. *J. Stat. Mech.* (2023) 093203
- [32] Potts, R. B.: Some generalized order-disorder transformations. *Proc. Cambridge Phil. Soc.* **48**, 106-109 (1952)
- [33] Fortuin, C. M., Kasteleyn, P. W.: On the random cluster model. *Physica* **57**, 536-564 (1972)
- [34] Wu, F. Y.: The Potts model. *Rev. Mod. Phys.* **54**, 235-268 (1982)
- [35] Pauling, L.: The structure and entropy of ice and other crystals with some randomness of atomic arrangement. *J. Am. Chem. Soc.* **57**, 2680-2684 (1935)
- [36] Nagle, J.F.: Lattice statistics of hydrogen-bonded crystals. I. the residual entropy of ice, *J. Math. Phys.* **7**, 1484-1491 (1966)
- [37] A. Lenard, cited in [38]
- [38] Lieb, E. H.: Residual entropy of square ice, *Phys. Rev.* **162**, 162-172 (1967)

- [39] Jakovac, J., Klavžar, S.: Vertex-, edge-, and total-colorings of Sierpinski-like graphs, *Discr. Math.* **309**, 1548-1556 (2009)
- [40] Hinz, A., Parisse, D.: Coloring Hanoi and Sierpinski graphs, *Discr. Math.* **312**, 1521-1535 (2012)
- [41] Hinz, A., Klavžar, S., Zemljič, S.: A survey and classification of Sierpinski-type graphs, *Discr. Appl. Math.* **217**, 565-600 (2017)
- [42] Chang, S.-C., Chen, L.-C.: Spanning trees on the Sierpinski gasket. *J. Stat. Phys.* **126**, 649 (2007)
- [43] Chang, S.-C., Chen, L.-C.: Spanning forests on the Sierpinski gasket. *J. Stat. Phys.* **126**, 649-667 (2007)
- [44] Chang, S.-C., Chen, L.-C.: Dimer coverings on the Sierpinski gasket. *J. Stat. Phys.* **131**, 631-650 (2008)
- [45] Chang, S.-C., Chen, L.-C.: Dimer-monomer model on the Sierpinski gasket. *Physica A* **387**, 1551–1566 (2008)
- [46] Chang, S.-C., Chen, L.-C.: Connected spanning subgraphs on the Sierpinski gasket. *Discret. Math. Theor. Comput. Sci.* **11**, 55-78 (2009)
- [47] Chang, S.-C., Chen, L.-C.: Hamiltonian walks on the Sierpinski gasket. *J. Math. Phys.* **52**, 023301 (2011)
- [48] Chang, S.-C. Acyclic orientations on the Sierpinski gasket. *Int. J. Mod. Phys. B* **26**, 1250128 (2012)
- [49] Chang, S.-C., Chen, L.-C., Yan, W.: Asymptotic enumeration of independent sets on the Sierpinski gasket. *Filomat* **27**, 23-40 (2013)
- [50] Chen, H., Wu, R., Guang, G., Deng, H.: Dimer-monomer model on the towers of Hanoi graphs. *Int. J. Mod. Phys. B* **29**, 1550173 (2015)
- [51] Zhang, Z., Wu, S., Li, M., Comellas, F.: The number and degree distribution of spanning trees in the tower of Hanoi graph. *Theor. Comput. Sci.* **609**, 443–55 (2016)
- [52] Chen, H., Wu, R., Huang, G., Deng, H.: 2017 Independent sets on the towers of Hanoi graphs *Ars Math. Contemp.* **12**, 247–260 (2017)

- [53] Li, W.-B., Chang, S.-C.: Dimer coverings on the Tower of Hanoi graph. *Int. J. Mod. Phys. B* **33**, 1950043 (2019)
- [54] Li, W.-B., Chang, S.-C.: Study of monomer-dimer on the generalized Hanoi graph. *Comput. and Appl. Math*, **39**, 77 (2020)
- [55] Biggs, N.: *Algebraic Graph Theory*. Cambridge University Press, Cambridge (1993)
- [56] Bollobás, B.: *Modern Graph Theory*. Springer, New York (1998)
- [57] Dong, F. M., Koh, K. M., Teo, K. L., *Chromatic Polynomials and Chromaticity of Graphs*. World Scientific, Singapore (2005)
- [58] Shrock, R., Tsai, S.-H.: Asymptotic limits and zeros of chromatic polynomials and ground state entropy of Potts antiferromagnets. *Phys. Rev. E* **55**, 5165-5179 (1997)
- [59] Shrock, R. Exact Potts model partition functions for ladder graphs. *Physica A* **283**, 388-446 (2000)
- [60] Tutte, W. T.: A contribution to the theory of chromatic polynomials, *Canad. J. Math*, **6**, 80-91 (1954)
- [61] Tutte, W. T.: On Dichromatic polynomials, *J. Combin. Theory* **2**, 301-320 (1967)
- [62] Read, R. C., Tutte, W. T.: Chromatic polynomials. In: Beineke, L. W. and Wilson, R. J. (eds.), *Selected Topics in Graph Theory 3*, Academic Press, New York (1988), pp. 15-42
- [63] Brylawski, T. and Oxley, J.: The Tutte polynomial and its applications, in *Matroid Applications*. In: White (ed.), *Encyclopedia of Mathematics and its Applications*, ed. , Cambridge Univ. Press, Cambridge, UK (1992), pp. 123-225
- [64] Baxter, R. J.: Colorings of a hexagonal lattice. *J. Math. Phys.* **11**, 784-789 (1970)
- [65] Biggs, N. L., Damerell, R. M., Sands, D. A.: Recursive families of graphs. *J. Combin. Theory B* **12**, 123-131 (1972)
- [66] Biggs, N.: Colouring square lattice graphs. *Bull. London Math. Soc.* **9**, 54-56 (1977)
- [67] Kim, D., Enting, I. G.: The limit of chromatic polynomials. *J. Combin Theory Ser. B* **26**, 327-336 (1979)
- [68] Baxter, R. J.: q -Colourings of the triangular lattice. *J. Phys. A* **19**, 2821-2839 (1986)

- [69] Baxter, R. J.: Chromatic polynomials of large triangular lattices. *J. Phys. A* **20**, 5241-5261 (1987)
- [70] Mattis, D. C.: The q -Color problem on a lattice. *Int. J. Mod. Phys. B* **1**, 103-109 (1987).
- [71] Read, R. C., Royle, G. F.: Chromatic roots of families of graphs, in *Graph Theory, Combinatorics, and Applications*. In: Alavi, Y., Chartrand, G., Ollermann, O. R., Schwenk, A. J. (eds.). Wiley, New York, (1991)
- [72] Shrock, R., Tsai, S.-H.: Ground State Entropy and the $q = 3$ Potts Antiferromagnet on the Honeycomb Lattice. *J. Phys. A* **30**, 495-500 (1997)
- [73] Shrock, R., Tsai, S.-H.: Upper and lower bounds for ground state entropy of antiferromagnetic Potts models. *Phys. Rev. E* **55**, 6791-6794 (1997)
- [74] Shrock, R., Tsai, S.-H.: R. Shrock, S.-H. Tsai, Ground state entropy of Potts antiferromagnets: bounds, series, and Monte Carlo measurements. *Phys. Rev. E* **56**, 2733-2737 (1997)
- [75] Shrock, R., Tsai, S.-H.: Lower bounds and series for the ground state entropy of the Potts antiferromagnet on archimedean lattices and their duals. *Phys. Rev. E* **56**, 4111-4124 (1997)
- [76] Roček, M., Shrock, R., Tsai, S.-H.: Chromatic polynomials for families of strip graphs and their asymptotic limits. *Physica A* **252**, 505-546 (1998)
- [77] Shrock, R., Tsai, S.-H.: Ground state entropy of the Potts antiferromagnet on cyclic strip graphs. *J. Phys. A Letts.* **32**, L195-L200 (1999)
- [78] Shrock, R., Tsai, S.-H.: Ground state entropy of Potts antiferromagnets on cyclic polygon chain graphs. *J. Phys. A* **32**, 5053-5070 (1999)
- [79] Shrock, R., Tsai, S.-H.: Ground state degeneracy of Potts antiferromagnets on 2D lattices: approach using infinite cyclic strip graphs. *Phys. Rev.* **E60**, 3512-3515 (1999)
- [80] Shrock, R.: $T = 0$ Partition functions for Potts antiferromagnets on Möbius strips and effects of graph topology. *Phys. Lett. A* **261**, 57-62 (1999)
- [81] Biggs, N. L., Shrock, R.: $T = 0$ Partition functions for Potts antiferromagnets on square lattice strips with (twisted) periodic boundary conditions. *J. Phys. A (Letts)* **32**, L489-L493 (1999)

- [82] Shrock, R., Tsai, S.-H.: Exact partition functions for Potts antiferromagnets on cyclic lattice strips. *Physica A* **275**, 429-449 (2000)
- [83] Chang, S.-C., Shrock, R.: Ground State Entropy of the Potts Antiferromagnet on Strips of the Square Lattice. *Physica A* **290**, 402-430 (2001)
- [84] Chang, S.-C., Shrock, R.: Exact Potts model partition functions on wider arbitrary-length strips of the square lattice. *Physica A* **296**, 234-288 (2001)
- [85] Chang, S.-C., Shrock, R.: Exact Potts model partition functions on strips of the honeycomb lattice. *Physica A* **296**, 183-233 (2001)
- [86] Salas, J., Shrock, R.: Exact $T = 0$ partition functions for Potts antiferromagnets on sections of the simple cubic lattice. *Phys. Rev. E* **64**, 011111 (2001)
- [87] Chang, S.-C., Shrock, R.: Ground state entropy of the Potts antiferromagnet on triangular lattice strips. *Ann. Phys.* **290**, 124-155 (2001)
- [88] Chang, S.-C., Shrock, R.: Exact Potts model partition functions on strips of the triangular lattice. *Physica A* **286**, 189-238 (2000)
- [89] Chang, S.-C., Shrock, R.: $T = 0$ Partition functions for Potts antiferromagnets on lattice strips with fully periodic boundary conditions. *Physica A* **292**, 307-345 (2001)
- [90] Chang, S.-C., Shrock, R.: Potts model partition functions for self-dual families of graphs. *Physica A* **301**, 301-329 (2001)
- [91] Chang, S.-C., Shrock, R.: Complex-temperature phase diagrams for the q -state Potts model on self-dual families of graphs and the nature of the $q \rightarrow \infty$ limit. *Phys. Rev. E* **64**, 066116 (2001)
- [92] Salas, J., Sokal, A. D.: Transfer matrices and partition-function zeros for antiferromagnetic Potts models. I. General theory and square-lattice chromatic polynomial. *J. Stat. Phys.* **104**, 609-699 (2001)
- [93] Sokal, A. D.: Bounds on the complex zeros of (di)chromatic polynomials and Potts-model partition functions. *Combin. Probab. Comput.* **10**, 41-77 (2001)
- [94] Chang, S.-C., Shrock, R.: S.-C. Chang and R. Shrock, General Structural results for Potts model partition functions on lattice strips. *Physica A* **316**, 335-379 (2002)

- [95] Chang, S.-C., Salas, J., Shrock, R.: Exact Potts model partition functions for strips of the square lattice. *J. Stat. Phys.* **107**, 1207–1253, (2002)
- [96] Biggs, N.: Equimodular curves, *Discr. Math.* **259**, 37-57 (2002)
- [97] Jacobsen, J., Salas, J., Sokal, A. D.: Transfer matrices and partition-function zeros for anti-ferromagnetic Potts models. III. Triangular lattice chromatic polynomial, *J. Stat..Phys.* **112**, 921-1017 (2003)
- [98] Chang, S.-C., Jacobsen, J., Salas, J., Shrock, R.: Exact Potts model partition functions for strips of the triangular lattice, *J. Stat. Phys.* **114**, 763-822 (2004)
- [99] Ellis-Monaghan, J. et al.: A Little statistical mechanics for the graph theorist. *Discr. Math.* **310**, 2037-2053 (2010)
- [100] Woodall, D. R.: Zeros of chromatic polynomials, in *Proc. of the Sixth British Combinatorial Conference*, ed. P. J. Cameron, Academic Press, New York, (1977), pp. 199-223
- [101] Jackson, B.: A zero-free interval for chromatic polynomials of graphs. *Combin. Probab. Comput.* **2**, 325-336 (1993)
- [102] Thomassen, C.: The zero-free intervals for chromatic polynomials of graphs, *Combin. Probab. Comput.* **6**, 497-506 (1997)
- [103] Feldman, H., Shrock, R., Tsai, S.-H.: Complex-temperature partition function zeros of the Potts model on the honeycomb and kagomé Lattices. *Phys. Rev.* **E57**, 1335-1346 (1998)
- [104] Feldmann, H., Guttmann, A. J., Jensen, I., Shrock, R., Tsai, S.-H.: Study of the Potts model on the honeycomb and triangular lattices: low-temperature series and partition function zeros. *J. Phys. A* **31** 2287-2310 (1998)
- [105] Tutte, W. T.: On chromatic polynomials and the golden ratio. *J. Combin. Theory* **9**, 289-296 (1970)
- [106] Shrock, R., Xu, Y.: Chromatic polynomials of planar triangulations, the Tutte upper bound, and chromatic zeros. *J. Phys. A* **45**, 055212 (2012)
- [107] Shrock, R., Xu, Y.: The Structure of chromatic polynomials of planar triangulation graphs and implications for chromatic zeros and asymptotic limiting quantities. *J. Phys. A* **45**, 215202 (2012)

- [108] Yang, C. N., Lee, T. D.: Statistical theory of equations of state and phase transitions. I. Theory of condensation, Phys. Rev. **87**, 404-409 (1952)
- [109] Lee, T. D., Yang, C. N.: Statistical theory of equations of state and phase transitions. II. Lattice gas and Ising model, Phys. Rev. **87**, 410-419 (1952)
- [110] Fisher, M. E.: The nature of critical points. In: Lectures in Theoretical Physics. Brittin, W. E. (ed.) Univ. of Colorado Press, Boulder, vol. 12C (1965), pp. 1-159
- [111] Matveev, V., Shrock, R.: Complex-temperature singularities in Potts models on the square lattice. Phys. Rev. E **54**, 6174-6185 (1996).
- [112] Huang, H. Y., Wu, F. Y.: The infinite-state Potts model and partitions of an integer. Int. J. Mod. Phys. B **11**, 121-126 (1997)
- [113] Chang, S.-C., Shrock, R.: Zeros of the Potts Model Partition Function in the Large- q Limit, Int. J. Mod. Phys. B **21**, 979-994 (2007)